ADDIS ABABA UNIVERSITY

ADDIS ABABA INSTITUTE OF TECHNOLOGY

SCHOOL OF CIVIL AND ENVIRONMENTAL ENGINEERING

Parametric Study of Gabled Hyperbolic Paraboloid Reinforced Concrete Shell Roof

---

A Thesis in Structural Engineering

By Ibsa Nugusa

October 2019

Addis Ababa

A Thesis

Submitted in Partial Fulfillment of the Requirements for the Degree of Master of Science

The undersigned have examined the thesis entitled '**Parametric Study of Gabled Hyperbolic Paraboloid Reinforced Concrete Shell Roof**' presented by **IBSA NUGUSA**, a candidate for the degree of **Master of Science** and hereby certify that it is worthy of acceptance.

Dr. Shifferaw Taye		
Advisor	Signature	Date
Internal Examiner	Signature	Date
External Examiner	Signature	Date
Chair person	Signature	Date

UNDERTAKING

I certify that research work titled “Parametric Study of Gabled Hyperbolic Paraboloid Reinforced Concrete Shell Roof” is my own work. The work has not been presented elsewhere for assessment. Where material has been used from other sources it has been properly acknowledged / referred.

Ibsa Nugusa

ABSTRACT

The structural behavior of the gabled hyperbolic paraboloid (hypar) reinforced concrete shell roof is investigated to use it efficiently. To attain this purpose, the parametric study of the gabled hypar reinforced concrete shell is carried out using the finite element software package SAP2000. From the analysis result membrane shear force increase with increasing shell ratio of the side, shell thickness, ridge beam depth and width, tie beam width, shell and ridge beam concrete class, and decreasing shell rise to span ratio, edge beam depth and width, edge and ridge beam concrete class. Moreover, the displacement increase as shell ratio of the side, ridge beam depth and width and tie beam width increase, and shell rise to span ratio, shell thickness, edge beam depth and width, shell, edge beam and ridge beam concrete class decrease.

ACKNOWLEDGMENTS

First of all, I would like to thank the Almighty God for his wonderful grace to carry me through. Next, I would like to express my gratitude to Ethiopian Road Authority (ERA) for the scholarship offer and Addis Ababa University for selecting me for this study. Thirdly, I want to express my deepest appreciation to my advisor, Dr. Shifferaw Taye, for his inspiration, valuable advice, invaluable suggestions and thorough guidance throughout the work of this thesis. Finally, I would like to give my special thanks for my families and friends for their continuous support and encouragement throughout this thesis.

TABLE OF CONTENTS

LIST OF FIGURES

LIST OF ABBREVIATIONS AND SYMBOLS

a	half of the hypar shell span (length)
b	half of the hypar shell width
D	membrane stiffness
d_{sx}	length of the section along x-axis
d_{sy}	length of the section along y-axis
E	effects of actions
Ed	design value of effect of actions
ERA	Ethiopian Road Authority
F_E	axial force in the boundary members
FEM	finite element method
Gk,j	characteristics value of permanent actions, j
h	shell rise
Hypar	hyperbolic paraboloid
l	curvature of the surface in the x-direction
m	torsion of the shell surface
M_x	bending moment along x-axis
M_{xy}	bending moment along xy-axis
M_y	bending moment along y-axis
M_{yx}	bending moment along yx-axis
n	curvature of the surface in the y-direction
N_x	membrane normal force along x-axis
N_{xy}	membrane shear force along xy-axis
N_y	membrane normal force along y-axis
N_{yx}	membrane shear force along yx-axis
P	load on the hypar shell
Px	load on the x-axis
Py	load on the y-axis
Pz	load on the z-axis
Qk,i	characteristics value of the accompanying variable action i
Q_x	shear force (out-of-plane) along x-axis
Q_y	shear force (out-of-plane) along y-axis

r	radius
r_x	radius of the section along x-axis
r_y	radius of the section along y-axis
S	length of the edge members
t	shell thickness
u	displacement component
v	displacement component
w	displacement component
X_x	displacement gradient in the x-axis
X_y	displacement gradient in the y-axis
X_{xy}	displacement gradient in the xy-axis
y1	location of maximum bending moment from edge
σ_x	normal stress along x-axis
σ_y	normal stress along y-axis
σ_{xy}	shear stress along xy-axis
σ_{yx}	shear stress along yx-axis
σ_{xz}	shear stress along xz-axis
σ_{yz}	shear stress along yz-axis
γsd	partial factor associated with the uncertainty of action and/ or action effect model
$\gamma g,j$	partial factor for permanent action, which takes account of the possibility of unfavorable deviations of the action from the representative values, j
γp	partial factors for pre-stressing action
γq,1	partial factor for variable actions, which takes into account of the possibility of unfavorable deviation of the actions values from the representative values, 1
$\gamma q,i$	partial factor for variable actions, which takes into account of the possibility of unfavorable deviation of the actions values from the representative values, i
γ_{xy}	strain in the xy-axis
ε_x	strain in the x-axis
ε_y	strain in the y-axis

ν	poisons ratio
τ	pure shear force
$\Psi 0,i$	factor for combination values of variable action i

CHAPTER 1 INTRODUCTION

Reinforced concrete thin shells can be defined as curved slabs whose thicknesses are small compared to their other dimensions like radius of curvature. Translational shell middle surface obtained by the translation of a moving plane curve over another stationary curve. Paraboloid shells are translational shells formed from two parabolas placed at right angle to each other and by translation of one parabola over the other.

Hyperbolic paraboloid (Hypar) shells are one group of paraboloid shell that formed by doubly curved shells with negative Gaussian curvature that is non-developable surface. A hypar surface generated by sliding a concave parabola on another plane, but convex, parabolic curve. Hypars are often combined to produce what are commonly known as umbrella shells. The most common types of umbrella shells are hipped- and inverted-type umbrella shells. The hipped umbrella roof, otherwise known as gabled hypar, and supported by four columns consists of four hypars resting on four diaphragms along their edges.

Hypar shells are structurally efficient and many constructional and aesthetic advantages. The use of reinforced concrete in the hypar offers the same advantages inherent to all shells of this material such as lightness, incombustibility, economy of materials, security against impact, and little sensitiveness to foundation settlement.

1.1 Statement of the Problem

Almost all the designer uses software packages based on finite element analysis for structural analysis. Accordingly, the designer should understand the behavior of the structural to minimize the efforts in modeling the structure and obtain the optimum section. However, limited number of researches is carried out on structural behavior of gabled hypar reinforced concrete shell. Moreover, since it carry loads mainly from the geometric features; to optimize the structural performance parametric study necessary. Thus, the intension of this thesis to study the behavior of reinforced concrete gabled hypar shell by varying its parameters to discuss on the effect these parameters.

1.2 Objectives

The main objective of this thesis is to study the structural behavior of gabled hypar reinforced concrete shell roof under the variation parameters.

1.3 Scope

This thesis covers the parametric study of reinforced concrete gabled hypar shell roof that include rise to span ratio, ratio of the side (length to width ratio) and thickness from shell geometry, depth and width of the edge beam, ridge beam and tie beam from the beam dimension, and concrete grade of the shell and beams from material properties. The actions included are self-weight and imposed load.

1.4 Methodology

This thesis will primarily employ quantitative research methods (i.e. structural analysis) aimed to study the parameters influencing the structural behavior of the gabled hypar shell roof. The following procedures are used to accomplish the objective of this thesis.

1.4.1 Selecting the parameters

Selection of the parameters affecting the structural performance of the gabled hypar reinforced concrete shell based on the literature review.

1.4.2 Modeling and analysis

The modeling and analysis of the structure includes:

- Determination of the load on the structure
- Verification of the numerical analysis done by finite element software package SAP2000 version 20.2.0 using analytical analysis taken from literature review by selected samples
- Modelling and analysis the structures sufficient samples for selected cases

1.4.3 Discussion of the analysis result

Discussion on the analysis result obtained for selected cases using graphic form that shows variable against the response of the structure.

1.4.4 Conclusion and recommendation

Concluding the discussion of the analysis result and recommending on how to use the selected parameters efficiently and the future research areas on the gabled hypar reinforced concrete shell is provided.

1.5 Organization of Thesis

This thesis is organized into five chapters. Chapter one is an introduction that contains the statement of the problem, objectives, scope, research approach and organization of thesis. A literature review of the method of analysis of gabled hypar shells and parameters influencing its behavior is stated in Chapter two. Chapter three is about the modelling and analysis of the shell which include selection of the parameters to be studied, computation of the actions on the structure, verification of the finite element method (FEM) and analysis of the structure. Analysis results and the discussion on these analysis results are presented in chapter four. Finally, in Chapter five, the conclusions and recommendations are given.

CHAPTER 2 LITERATURE REVIEW

2.1 Introduction

Reinforced concrete thin shells can be defined as curved slabs whose thicknesses are small compared to their other dimensions like radius of curvature. Translational shell middle surface obtained by the translation of a moving plane curve, called the generator (generatrix), which moves parallel to itself over another stationary curve, called the directrix (the function of these being interchangeable)[1].

Paraboloid shells are translational shells formed from two parabolas placed at right angle to each other and by translation of one parabola over the other. The common paraboloids may be subdivided into the following three groups [1]:

- Elliptical paraboloid: is formed by two unequal parabolas with same curvature sign (both convex in the same directions)
- Circular paraboloid: is formed by two equal parabolas with same curvature sign (both concave curved in the same direction)
- Hyperbolic paraboloid: is formed by two parabolas of opposite curvatures (one convex and the other concave in the opposite directions)

Hypar shells are doubly curved shells with negative Gaussian curvature that is non-developable surface. A hypar surface is generated by sliding a concave parabola on another plane, but convex, parabolic curve. Hypar shells are structurally efficient and many constructional and aesthetic advantages: they are used to cover large spans, vast roofed areas, and a variety of other roofed spaces; they are used as foundations for special structures; they can be prefabricated simply [2]. The use of reinforced concrete in the hypar offers the same advantages inherent to all shells of this material such as lightness, incombustibility, economy of materials, security against impact, and little sensitiveness to foundation settlement [3].

Principally, we get two types of hypar. The first is the one bounded by curved lines which is a simple surface obtained by one parabola moving over another parabola used commonly as precast large span roof elements for storage sheds, factories, etc. The second type

bounded by straight lines (with edges parallel to generators) is got by change of axis, which is a ruled surface (or a warped surface) with straight edges. Because of its ease in construction of formwork, it is nowadays very popular for large span buildings such as assembly halls and exhibition halls [1].

Hypar are often combined to produce what are commonly known as umbrella shells. If the alignment takes place along the characteristics straight lines, they are joined along an axis of symmetry. The most common types of umbrella shells are hipped- and inverted-type umbrella shells [4].

The hipped umbrella roof, otherwise known as gabled hypar, and supported by four columns is shown in the figure 2.1, consists of four hypars resting on four diaphragms along their edges as shown in figure 2.1[4].

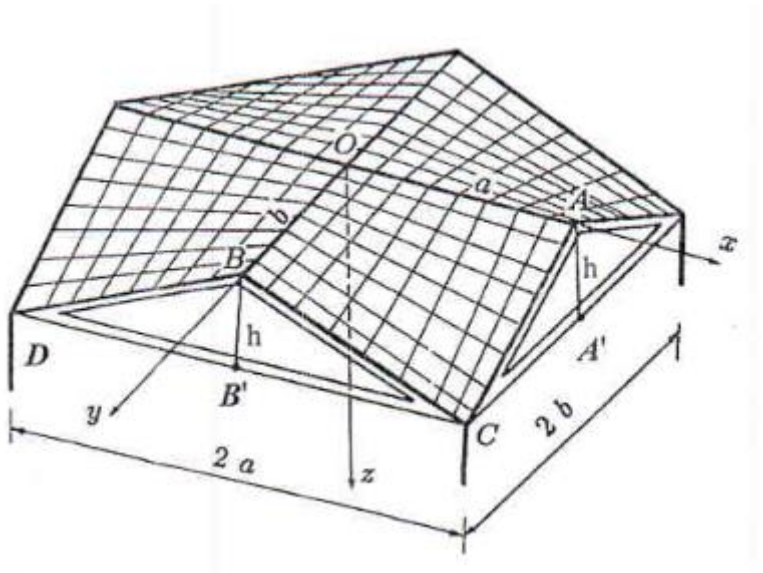

Figure 1. Gabled hypar shell

Shell panels have zero curvature along the direction of the perimeter but have convex or concave surfaces along the diagonal direction. In general, beams are located at the boundaries of shell panels. The beams located along the sloping lines of shell panels are referred to as edge beams, and beams located along the straight lines where the shell panels meet are called ridge or crown beams [5].

A proper design of hypars depends up on:

- A correct overall picture of behavior as diagonal compression arches
- A sufficient curvature at mid span to keep stresses low
- A stiffening of the flat central part by reinforcement and properly placed ribs that are no heavier than necessary
- Sufficient stiffness at the supports to prevent horizontal displacements

In such shells a major question will be creep and large mid span deflections all contributing to buckling [6].

2.2 Structural Analysis

The behavior of shell structures is different from that of so-called "framed structures". This feature originates mainly from the geometrical features of shells which make the internal force distribution in shells is three dimensional, i.e., spatial. Moreover, shell structures carry the applied forces mostly by the so-called membrane forces, whereas other structural forms carry the applied loads by bending mechanisms [2].

The structural analysis of thin concrete shells can be conducted analytically based on classical theory of thin shells or/and numerically using finite element analysis [7].

2.2.1 Analytical analysis

When different mathematical techniques are used to develop a response to a mathematical model of a structure, the solution is called an analytical solution. It is a mathematical expression gives the value of the field variable at any location and any circumstances in the body [7], [8].

2.2.1.1 Internal force system in a shell

Consider a shell with a general geometry. An infinitesimal element of this shell can be cutout by intersecting it with two pairs of principal plane sections which are located at are lengths d_{sx} and d_{sy} apart. Two intersecting planes are from each pair the normal to the shell at the common corner point. The resulting plane curves of intersection are principal sections and are thus perpendicular to each other (figure 2). The principal plane curve shapes principal radii of curvature that, in this figure, are designated by r_x and r_y [2].

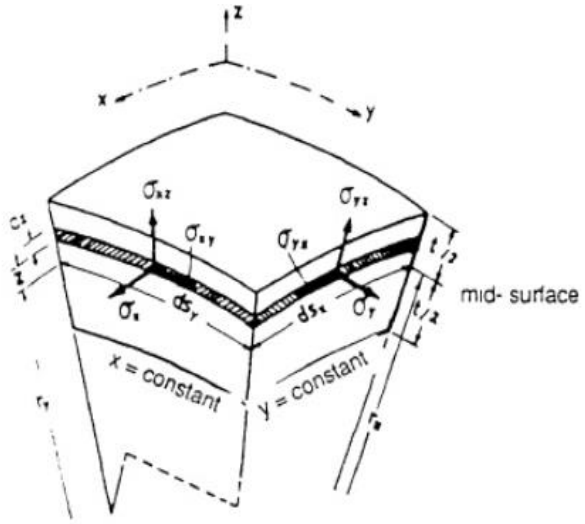

Figure 2. Principal radii of curvature and the internal stresses

In a shell structure subjected to applied external loading, temperature changes, support settlements, and deformation constraints, some internal stresses may develop. These internal stresses are shown on the shell element of figure 3. As we see, the general state of stress in a shell element consists of membrane normal and shear stresses lying in the shell surface, as well as the transverse shear stresses. In thin shells, the component of stress normal to the shell surface, compared with other components of the internal stresses, is very small and is neglected in the c1assical shell theories [2].

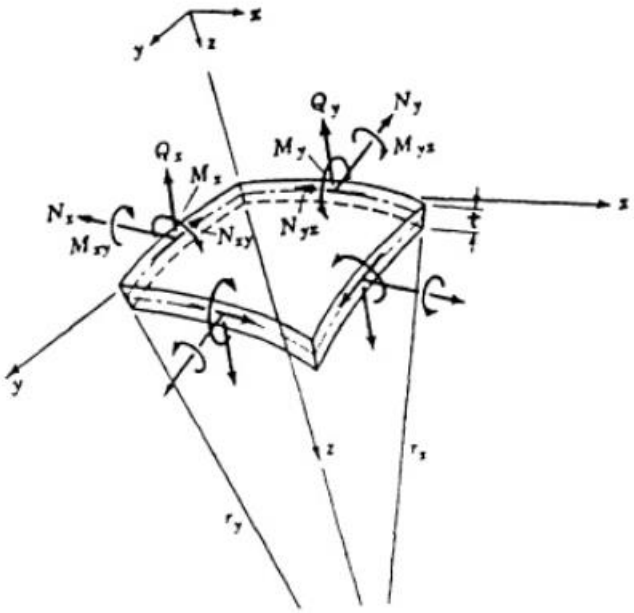

Figure 3. Components of internal force resultants in a shell element

Referring to figure 2, we can readily derive the relations between stress components and components of internal force resultant in a shell element. The desired relations have been obtained using the requirement of statical equivalency between the internal stresses and their resultant forces. In these relations, t is the thickness of the shell [2].

$$N_x = \int_{-\frac{t}{2}}^{+\frac{t}{2}} \sigma_x \left(1 + \frac{z}{r_y}\right) d_z, \quad N_y = \int_{-\frac{t}{2}}^{+\frac{t}{2}} \sigma_y \left(1 + \frac{z}{r_x}\right) d_z, \quad \text{..... 1(a)}$$

$$N_{xy} = \int_{-\frac{t}{2}}^{+\frac{t}{2}} \sigma_{xy} \left(1 + \frac{z}{r_y}\right) d_z, \; N_{yx} = \int_{-\frac{t}{2}}^{+\frac{t}{2}} \sigma_{yx} \left(1 + \frac{z}{r_x}\right) d_z \quad \text{.....1(b)}$$

$$Q_x = \int_{-\frac{t}{2}}^{+\frac{t}{2}} \sigma_{xz} \left(1 + \frac{z}{r_y}\right) d_z, \; Q_y = \int_{-\frac{t}{2}}^{+\frac{t}{2}} \sigma_{yz} \left(1 + \frac{z}{r_x}\right) d_z \quad \text{.....1(c)}$$

$$M_x = \int_{-\frac{t}{2}}^{+\frac{t}{2}} z\sigma_x \left(1 + \frac{z}{r_y}\right) d_z, \quad M_y = \int_{-\frac{t}{2}}^{+\frac{t}{2}} z\sigma_y \left(1 + \frac{z}{r_x}\right) d_z \quad \text{.....1(d)}$$

$$M_{xy} = -\int_{-\frac{t}{2}}^{+\frac{t}{2}} z\sigma_{xy} \left(1 + \frac{z}{r_y}\right) d_z, \quad M_{yx} = \int_{-\frac{t}{2}}^{+\frac{t}{2}} z\sigma_{yx} \left(1 + \frac{z}{r_x}\right) d_z \quad \text{.....1(e)}$$

where: N_x - membrane normal force along x-axis

σ_x - normal stress along x-axis

N_y - membrane normal force along y-axis

N_{xy} - membrane shear force along xy-axis

N_{yx} - membrane shear force along yx-axis

Q_x - shear force (out-of-plane) along x-axis

σ_y - normal stress along y-axis

σ_{xy} - shear stress along xy-axis

σ_{yx} - shear stress along yx-axis

Q_x - shear force (out-of-plane) along x-axis

Q_y - shear force (out-of-plane) along y-axis

M_x - bending moment along x-axis

M_y - bending moment along y-axis

M_{xy} - bending moment along xy-axis

M_{yx} - bending moment along yx-axis

The internal forces at each point of the shell may be placed in one of two groups of force fields: membrane forces and bending forces. The membrane forces are the resultant internal forces which lie "inside" the mid-surface of the shell. The membrane force field causes the stretching or contraction of the shell, as a membrane, without producing any bending and local curvature changes. The membrane force field consists of two membrane normal resultant forces and a membrane shear force. The second groups of internal forces are called the bending forces, since they cause bending and twisting of the shell cross-sections. The bending force field consists of bending moments, twisting couples, and transverse shear forces [2].

2.2.1.2 Qualitative description of shell behavior

The load-carrying mechanism, i.e., the internal forces at any point of a shell, consist of ten component internal force resultants (Nx, Ny, Nxy, Nyx, Mx, My, Mxy, Myx, Qx, Qy). These components can be separated into two groups, entitled membrane and bending internal force field, as follows [2]:

- Membrane field: Nx, Ny, Nxy, Nyx
- Bending field: Mx, My, Mxy, Myx, Qx, Qy

For a material body in spatial equilibrium there are six governing equilibrium equations. Since there are more than six force resultants, we conclude that a shell is, in general, an internally statically indeterminate structure. The internal force redundancy, although it is an indication of additional load carrying mechanisms, is not always required for shell equilibrium [2].

Let us imagine a shell subjected to applied loading in which only the membrane force field has been produced and the bending field is absent. By writing the moment equation of equilibrium about the normal to the shell element (z axis) we can conclude that Nxy =Nyx. Therefore, the membrane force field will consist of the forces Nx, Ny, and Nxy=Nyx. In a shell in which only the membrane field exists, three of the six equilibrium moment equations (Mx =0, My= 0, Mz=0) are identically satisfied [2].

We are then left with three remaining force equilibrium equations and three internal membrane forces to be determined. Since the number of equilibrium equations and

the number of unknown forces are equal, the membrane shell is statically determinate. The membrane force fields are associated with the membrane normal and shear forces, which are assumed to be uniformly distributed through the thickness of the shell. A shell in which only the membrane force field exists is said to have a membrane behavior. The resulting theory is called the membrane theory of shells [2].

The membrane field of forces and deformations will not, by themselves, be sufficient to satisfy all equilibrium and/or displacement requirements in the regions of equilibrium unconformity, geometrical incompatibility, loading discontinuity and geometrical non-uniformity. In these circumstances, some (or all) of the bending force field components are produced and, by being activated in those regions, compensate for the shortcomings of the membrane field in the disturbed zone [2].

The bending forces, being confined to a small region, leave the rest of the shell virtually free of bending actions. Therefore, in most cases, the major part of a shell structure behaves as a true membrane. This very interesting and unique character of shells is the result of the inherent curvature in the spatial shell form. It is this salient feature of shells that is responsible for the most profound and efficient structural performance of shells observed in nature [2].

2.2.1.3 Membrane analysis of hyperbolic paraboloid shells

Consider a straightedge hypar shell with the mid-surface equation of the form, [2]

$$z = \frac{xy}{h} = \frac{f}{ab}\,xy \quad \text{.....2}$$

in which

$$f = \frac{a^2}{b} \quad \text{.....3}$$

We use the governing membrane differential equation [2].

$$L(\dots) = \frac{r_2}{{r_1}^2}\frac{d^2(\dots)}{d\emptyset^2} + \frac{1}{r_1}\left[\frac{d}{d\emptyset}\left(\frac{r_2}{r_1}\right) + \frac{r_2}{r_1}\,cot\emptyset\right]\frac{d(\dots)}{d\emptyset} - \frac{r_1 cot^2\emptyset}{r_1 r_2}(\dots) \quad \text{.....4}$$

If we evaluate the second-order derivatives of z(x,y) and substitute them into the equation (4) , we obtain the following equation: [2]

$$-\frac{2}{h}\frac{\partial^2 \emptyset}{\partial x \partial y} = -p'_z + \frac{y}{h}P'_x + \frac{x}{h}p'_y \quad \text{.....5}$$

To carry out the analysis further, we must now specify the applied loading. Suppose that the shell is subjected to a load uniformly distributed with intensity P on the horizontal projection. In this case, the equation (5) becomes [2]

$$\frac{\partial^2 \emptyset}{\partial x \partial y} = \frac{1}{2}hP \quad \text{.....6}$$

This can easily be integrated twice with respect to x and y, to give [2]

$$\emptyset\,(x,y) = \frac{1}{2}hPxy + F_1(x) + F_2\,(y) \quad \text{.....7}$$

Here, $F_1(x)$ and $F_2(y)$ are two integration functions to be determined from the boundary conditions. We introduce a generating function, Ø(x,y), called the stress function and we define it as follows: [2]

$$N'_x = \frac{\partial^2 \emptyset}{\partial y^2} - \int P'_x\,dx \quad \text{.....8(a)}$$

$$N'_y = \frac{\partial^2 \emptyset}{\partial x^2} - \int P'_y\,dy \quad \text{.....8(b)}$$

$$N'_{xy} = -\frac{\partial^2 \emptyset}{\partial x \partial y} \quad \text{.....8(c)}$$

Now, the internal forces are given by the equation: [2]

$$N'_{xy} = -\frac{1}{2}hP = -\frac{ab}{2f}P \quad \text{.....9(a)}$$

$$N'_x = \sqrt{\frac{h^2+y^2}{h^2+x^2}}\,\frac{d^2F_2}{dy^2} \quad \text{.....9(b)}$$

$$N'_y = \sqrt{\frac{h^2+x^2}{h^2+y^2}}\,\frac{d^2F_1}{dx^2} \quad \text{.....9(c)}$$

The two sets of forces, Le. , the actual membrane forces (Nx, Ny & Nxy) and their plane-stress projections (Nx, Ny & Nxy), can be related using the shell geometry. We can write the relation between Nx and its horizontal projection (Nx) as [2]

$$N'_x dy = N_x dy\,\frac{cos\emptyset}{cos\Psi} \; or \; N_x = N'_x\sqrt{\frac{1+p^2}{1+q^2}} \quad \text{.....10}$$

in this relation,

$p = \frac{\partial z}{\partial x} = \tan \emptyset$ .....11(a)

$q = \frac{\partial z}{\partial y} = \tan \psi$ .....11(b)

In a similar fashion, we obtain [2]

$N_y = N'_y \sqrt{\frac{1+ q^2}{1+ p^2}}$ 12

and,

$N_{xy} = N'_{xy}$ 13

Using relations (6) to (13), we find

$N_{xy} = -\frac{1}{2} hp,\ N_x = \frac{d^2F_2}{dy^2},\ N_y = \frac{d^2F_1}{dx^2}$ 14

which shows that Nx is a function of y only, and Ny a function of x only [2].

A hypar shell may have a variety of edge conditions. In a majority of practical cases, edge members are comparatively stiff in their own plane, but cannot sustain loadings applied in the lateral direction, figure 4. In such cases, either or both of the normal forces, Nx and Ny, would vanish at the boundaries normal to their direction so that $F_1(x)$ and $F_2(y)$ would be assumed to be identically zero. Consequently, the normal membrane forces are identically zero throughout the shell and we are left with a pure shear membrane force field existing throughout the hypar shell [2].

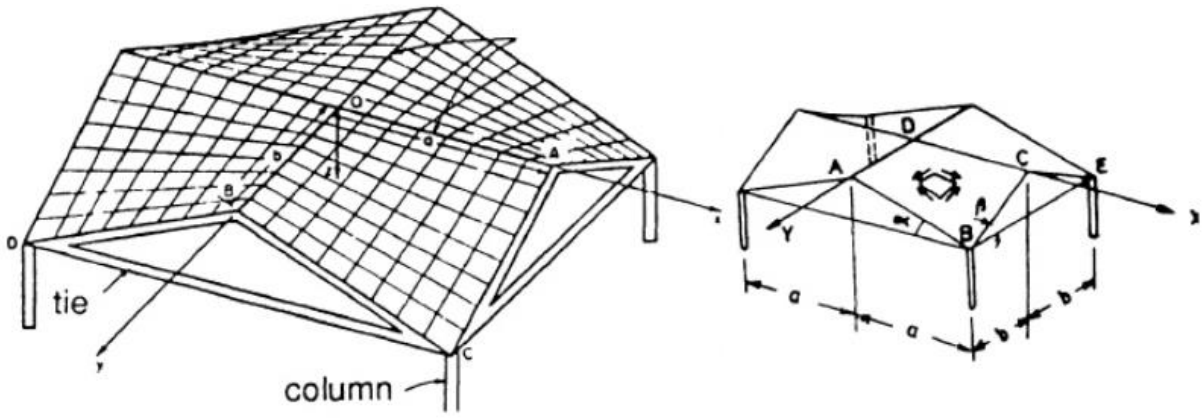

(a) (b)

Figure 4. Hypar shell composed of four hypar units resting on vertical corner supports

Consider the hypar shell roof shown in figure 4 (a), composed of four hypar shell segments. The whole shell structure rests at its four corners on vertical column supports. The applied loading is assumed to be uniformly distributed with intensity p on the horizontal projection of the shell [2].

The state of stress at a typical element of the shell is determined using relations (14) and the prescribed boundary conditions. The internal membrane force field along each generator line consists of a pure shear force of constant magnitude,

$$\tau = N_{xy} = -\frac{hp}{2} = -\frac{abp}{2f} \quad \text{.....15}$$

Figure 4 (b) shows the state of stress in an element of the shell. A more detailed picture of stress and force distribution in the shell is presented in figure (5) [2].

The principal stresses at any point corresponding to this pure shear are a tensile stress τ in the direction parallel to OB and a compressive stress τ in the direction parallel to AC [2].

According to membrane theory, there exists a distributed internal shear force system at the edges of the shell of figure 5. To satisfy the equilibrium requirements of membrane theory, these edge shears must be transferred to vertical supports by means of some intermediate members. Two types of such members are needed: edge beams and ridge beams; members such as AB and BC are edge beam, and AD and CD are ridge beams [2].

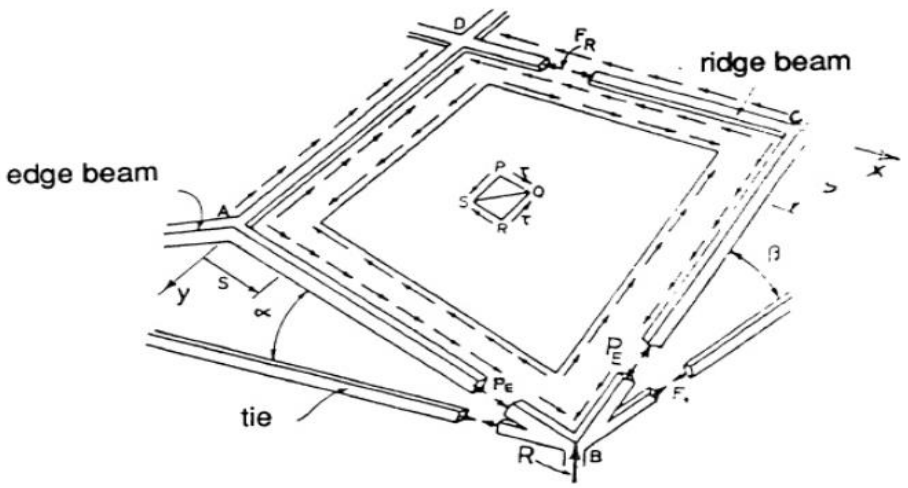

Figure 5. Internal force distribution in a segment of the hypar shell

The internal membrane shear force, C, in being transferred to the edge and ridge beams cause axial forces in those members. In the present case, figure 4 shows that the axial forces in both the edge beams and the ridge beam happen to be compressive. In other cases, either of these axial forces may be tensile [2].

The magnitudes of axial compressive forces in the boundary members of the shell of figure 4 are

$$(F_E)_{AB} = N_{xy}.S = N_{xy}\frac{x}{cos\alpha} = -\frac{ab}{2f}\frac{px}{cos\alpha} \quad \text{.....16 (a)}$$

$$(F_E)_{BC} = N_{xy}.S = N_{xy}\frac{y}{cos\beta} = -\frac{ab}{2f}\frac{py}{cos\beta} \quad \text{.....16 (b)}$$

At the corners of the structure, the edge beams produce axial thrusts as well as vertical forces. The vertical forces are carried by the vertical column supports, but the horizontal thrusts must be absorbed by tie members. Figure 4 shows horizontal ties carrying the axial thrust in tension [2].

The resultant of vertical forces at each corner, to be supported by the column, is

$$R = \frac{ab}{2f}\frac{pa}{cos\alpha}\,sin\alpha + \frac{ab}{2f}\frac{pb}{cos\beta}\,sin\beta = pab \quad \text{.....17}$$

and the axial compressive force in, for example, the ridge beam CD is equal to:

$$F_R = 2\,(a-x)N_{xy} = -h(a-x)p \quad \text{.....18}$$

As we see, the axial force of the ridge beam is zero at the outer boundary (the edge) and maximum at the center [2].

2.2.1.4 Description of membrane behavior of hyperbolic paraboloid shells

According to the membrane theory, the state of stress in a hypar shell element, oriented along the straight-edge generators, is a pure shear which remains constant throughout the shell. The principal stresses make 45° with the straight-line generators; one principal stress is tensile, the other compressive; both are constant throughout the shell. In hypar shells having edge members, the applied load is normally transferred to the edge and the ridge

beams which, in turn, carry the induced axial forces to the shell supports. Figures 6 show the flow of internal forces from the shell body to the edge members of the shells [2].

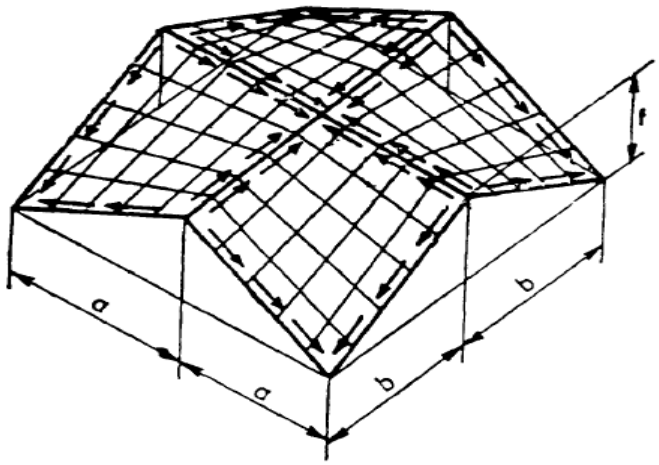

Figure 6. Transfer of internal forces to the edge members in some hypar shell

We conclude that the structural action of the hypar shell arises from the interaction of two mechanisms:

- a cable action of the shell along the directions of principal tensile stresses, and
- an arch action along the lines of maximum compressive stresses.

The sign of the axial force developed in the edge and ridge beams of hypar shells depends on the shell configuration and the supporting conditions [2].

2.2.1.5 Bending theory of shallow shells

The bending theory of general shells can be simplified to yield equations which can be solved analytically and numerically. One of such simplifications is the so-called "shallow shell theory", based on the assumptions [2]:

- The slope of the shell (root) is small.
- The curvature of the shell, as well as the changes in curvature of the shell, is small. As a guideline, the range of rise to span ratio of less than 1/5 is suggested for shallow shells.
- The loading as well as shell boundaries are such that the applied loads are carried primarily by the in-plane forces.

- The deformations normal to the shell surface are greater than the in plane deformations.

For practical purposes, many Hypar shells and also Conoidal shells may be considered to be shallow shells. This approximate theory is also referred to as Vlasov Theory of shallow shells [2].

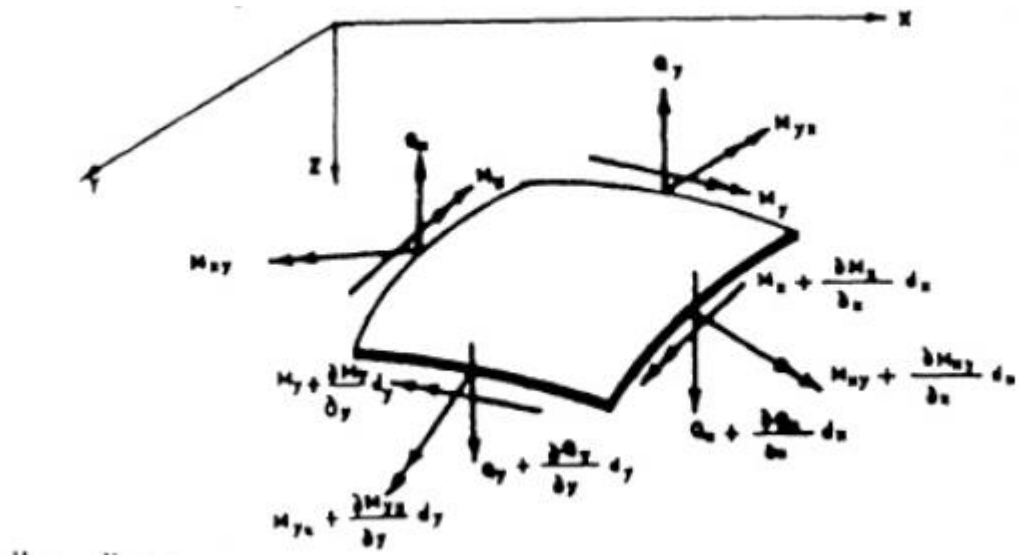

Figure 7. An element of an arbitrary shallow shell

Consider a shell with a general middle surface defined by the equation z = z(x,y) in an orthogonal Cartesian coordinate system. We have,

$$\frac{\partial^2 z}{\partial x^2} = l \quad \text{.....19(a)}$$

Curvature of the surface in the x-direction

$$\frac{\partial^2 z}{\partial x \partial y} = m \quad \text{.....19(b)}$$

Torsion of the shell surface

$$\frac{\partial^2 z}{\partial y^2} = n \quad \text{.....19(c)}$$

Curvature of the surface in y-direction

With these definitions and related interpretations, we now proceed to derive the governing equations of linearly elastic shallow shells [2].

a. Equations of equilibrium

Consider an infinitesimal element of a shallow shell. Figures 7 show the membrane and the bending fields of internal forces acting on this element. We assume that the shell is acted upon by a general distributed force having the components Px, Py, and pz along x, y, and z axes, respectively. In this treatment, z axis is assumed to lie along the vertical direction. Thus, x-y plane defines the horizontal surface [2].

The equilibrium equations have the following forms:

$$\frac{\partial N_x}{\partial x} + \frac{\partial N_{yx}}{\partial y} + Px = 0 \quad \text{.....20(a)}$$

Equilibrium of forces along x axis

$$\frac{\partial N_y}{\partial y} + \frac{\partial N_{xy}}{\partial x} + Py = 0 \quad \text{.....20(b)}$$

Equilibrium of forces along y axis

$$\frac{\partial Q_x}{\partial x} + \frac{\partial Q_y}{\partial y} + N_x \frac{\partial^2 z}{\partial x^2} + 2N_{xy} \frac{\partial^2 z}{\partial x \partial y} + N_y \frac{\partial^2 z}{\partial y^2} + P_z = 0 \quad \text{.....20(c)}$$

Equilibrium of forces along z axis

$$M_{yx} = -M_{xy} \quad \text{.....20(d)}$$

Equilibrium of moments about z axis

$$\frac{\partial M_y}{\partial y} + \frac{\partial M_{xy}}{\partial x} - Q_y = 0 \quad \text{.....20(e)}$$

Equilibrium of moments about x axis

$$\frac{\partial M_x}{\partial x} + \frac{\partial M_{xy}}{\partial y} - Q_x = 0 \quad \text{.....20(f)}$$

Equilibrium of moments about y axis

Equations (20 (e)) and (20 (f)) can be rewritten as,

$$Q_y = \frac{\partial M_y}{\partial y} + \frac{\partial M_{xy}}{\partial x} \quad \text{.....21(a)}$$

$$Q_x = \frac{\partial M_x}{\partial x} + \frac{\partial M_{xy}}{\partial y} \quad \text{.....21(b)}$$

If we substitute the expressions for Qx and Qy from these relations into (20 (c)) we obtain,

$$\frac{\partial^2 M_x}{\partial x^2} + 2\,\frac{\partial^2 M_y}{\partial x \partial y} + \frac{\partial^2 M_y}{\partial y^2} + N_x \frac{\partial^2 z}{\partial x^2} + 2N_{xy}\frac{\partial^2 z}{\partial x \partial y} + N_y \frac{\partial^2 z}{\partial y^2} + p_z = 0 \quad \text{.....22}$$

b. Kinematic relations

The displacement field of the mid-surface of the shell is assumed to have three components defined by the functions u, v, and w. Inspired by the corresponding relations for cylindrical shells, we assume the following strain-displacement relations for shallow shells [2].

$$\varepsilon_x = \frac{\partial u}{\partial x} - lw \quad \text{.....23(a)}$$

$$\varepsilon_y = \frac{\partial v}{\partial y} - nw \quad \text{.....23(b)}$$

$$\gamma_{xy} = \frac{\partial u}{\partial y} + \frac{\partial v}{\partial x} \quad \text{.....23(b)}$$

In these relations, ε_x, ε_y, γ_{xy} are the strain components of an arbitrary point in the shell thickness. As we note, in the present approximation, the influence of normal displacement component, w, (which in this approximate theory is assumed to be the same as vertical displacement) is highlighted. In other words, the gradients of other components are neglected in comparison with those of the function w [2].

The relations between the change in curvature and also the twist of the shell, on one hand, and the displacement gradients, on the other hand, are,

$$X_x = \frac{\partial^2 w}{\partial x^2} \quad \text{.....24(a)}$$

$$X_y = \frac{\partial^2 w}{\partial y^2} \quad \text{.....24(b)}$$

$$X_{xy} = \frac{\partial^2 w}{\partial x \partial y} \quad \text{.....24(c)}$$

These are the desired kinematic relations for shallow shells [2].

c. Constitutive relations

The constitutive relations for a linearly elastic and isotropic shallow shell, assuming the decoupling of membrane and bending relations can be expressed as follow:

$N_x = \frac{Et}{1-\nu^2}\ (\varepsilon_x + \nu\varepsilon_y)$ ……..……25(a)

$N_y = \frac{Et}{1-\theta^2}\ (X_y + \nu X_x)$ ……..……25(b)

$N_{xy} = N_{yx} = \frac{Et}{2(1+\nu)}\ X_{xy}$ ……....25(c)

$M_x = -k\ (X_x + \nu X_y)$ ……..……..25(d)

$M_y = -k\ (X_y + \nu X_y)$ ……..…….25(e)

$M_{xy} = -k\ (1-\nu)\ X_{xy}$ ……..……26(f)

In these relations, the parameters D and K are the membrane and bending stiffness of the shell, respectively [2].

$D = \frac{Et}{1-\nu^2} \quad k = \frac{Et}{12\ (1-\nu^2)}$ ……..27

By combining the three types of basic relations, Le., equilibrium, kinematic and constitutive relations we obtain the governing equations of Vlasov theory of shallow shells. The synthesis procedure is as follows [2]:

By differentiating both sides of relations (23(a) and 23(b)) twice, with respect to y and x respectively, and after adding up both sides of resulting relations, we obtain,

$\frac{\partial^2\varepsilon_x}{\partial y^2} + \frac{\partial^2\varepsilon_y}{\partial x^2} = \frac{\partial^2 u}{\partial x\partial y} + \frac{\partial^3 u}{\partial y\partial x^2} - l\frac{\partial^2 w}{\partial y^2} - n\frac{\partial^2 w}{\partial x^2}$ ……..28

and from the relation (23(c)),

$\frac{\partial^2\gamma_{xy}}{\partial x\partial y} = \frac{\partial^3 u}{\partial x\partial y^2} + \frac{\partial^3 u}{\partial y\partial x^2} - 2m\ \frac{\partial^2 w}{\partial x\partial y}$ ……..29

Now, by combing relations (28) and (29) we obtain

$\frac{\partial^2\varepsilon_x}{\partial y^2} + \frac{\partial^2\varepsilon_y}{\partial x^2} = \frac{\partial^2\gamma_{xy}}{\partial x\partial y} - l\ \frac{\partial^2 w}{\partial y^2} + 2m\ \frac{\partial^2 w}{\partial x\partial y} - n\frac{\partial^2 w}{\partial x^2}$ ……..30

At this stage, we consider special loading types in which only the applied loading has a vertical component Pz and the other loading components are identically zero. This is common for practical roof shell design problems [2].

To reduce the number of governing equations, we now introduce a stress function, Ø (x,y), and we define it in the following fashion:

$$N_x = \frac{\partial^2 \emptyset}{\partial y^2},\ N_y = \frac{\partial^2 \emptyset}{\partial x^2},\qquad N_{xy} = -\frac{\partial^2 \emptyset}{\partial x \partial y} \quad \text{.....31}$$

Also, we rewrite the equation (30) in the following form:

$$\left(\frac{\partial^2 \varepsilon_x}{\partial y^2} - \frac{\partial^2 \gamma_{xy}}{\partial x \partial y} + \frac{\partial^2 \varepsilon_{xy}}{\partial x^2}\right) + \left(l\frac{\partial^2 w}{\partial y^2} - 2S\ \frac{\partial^2 w}{\partial x \partial y} + m\ \frac{\partial^2 w}{\partial x^2}\right) = 0 \quad \text{.....32}$$

If we make use of constitutive relations (29), the strain displacement relations (23) and stress function relations (31) in the above relation, we obtain,

$$\nabla^4 \emptyset + Et{\nabla_k}^2 w = 0 \quad \text{.....33(a)}$$

$${\nabla_k}^2 \equiv (l\frac{\partial^2}{\partial x \partial y} - 2m\ \frac{\partial^2}{\partial x \partial y} + n\frac{\partial^2}{\partial x^2} \quad \text{.....33(b)}$$

In which,

$$\nabla^4 = \left(\frac{\partial^2}{\partial x^2} + \frac{\partial^2}{\partial y^2}\right)\left(\frac{\partial^2}{\partial x^2} + \frac{\partial^2}{\partial y^2}\right) = \frac{\partial^4}{\partial x^4} + 2\frac{\partial^4}{\partial x^2 \partial y^2} + \frac{\partial^4}{\partial y^4} \quad \text{.....34}$$

Now, substituting relations (25 (d)), (25 (e)), (25(f)) and also relations (28) and (31), into the equation (34), we obtain

$$-k\nabla^4 w + {\nabla_k}^2 \emptyset + P_z = 0\ or\ k\nabla^4 w - {\nabla_k}^2 = P_z \quad \text{.....35}$$

Equations (33) and (35) constitute the governing equations of Vlasov theory of shallow shells [2].

These equations for shallow shells contain more special theories as their off springs [2]:

1. **Theory of flat plates-**For a flat plate, the initial curvature is zero. In this case, the governing equations of shallow shells become decoup1ed and take the following forms:

$k\nabla^4 w = P_z,\ \nabla^2 \emptyset = 0$ ……...36

These equations govern a laterally loaded thin plate as well as the same plate loaded by in-plane forces and acting in plane stress.

2. **Membrane shallow shells-**In this ease, the bending stiffness of the shell, K, is assumed to be zero. The governing equation of this membrane shell is derived from shallow shell equations to be,

$\nabla^2 \emptyset = P_z$ ……..…….37

The governing field equations of shallow shells must be supplemented by appropriate boundary conditions. These equations can then be solved analytically by means of series expansions or otherwise. Numerical solution of shallow shell problems can be obtained by finite-element or finite-difference methods.

2.2.1.6 Bending field in hypar shells

The results of this section were obtained by Loof who has used Vlasov theory of shallow shells to find the bending field of moment and shear in the square hypar shells with straight line generators [2].

Loofs results for two different boundary conditions in a square hypar shells are as follows [2]:

1. **Shell with fixed edges**

$M_y = -0.511\ g a^2 \left(\frac{h}{t}\right)^{-\frac{4}{3}}$ ……..……38(a)

$Q_y = +1.732\ g\ a\ \left(\frac{f}{t}\right)^{-1}$ ……38(b)

In these formulas (38), My and Qy are the bending moment and the shear force in the mid-length of the shell edge. The parameter g represents the intensity of uniformly distributed vertical load; a stands for both width and length; h and t denote the rise and the thickness of the shell, respectively.

2. **Shell with hinged Edge**

The bending moment is zero but the non-zero transverse shear force is,

$$Q_y = +0.577\, g\, a \left(\frac{h}{t}\right)^{-1} \quad \text{.....39}$$

The maximum bending moment occurs at a section located at a distance y1 from the edge, where

$$y_1 = 0.55 \left(\frac{h}{t}\right)^{-\frac{1}{3}} a \quad \text{.....40}$$

and the corresponding bending moment is,

$$M_y = +0.149\, g\, a^2 \left(\frac{h}{t}\right)^{-\frac{4}{3}} \quad \text{.....41}$$

These formulas show that the bending moment is reduced by increasing the shell rise, and increased by increasing the shell thickness.

2.2.2 Numerical analysis

For problems involving complex boundary conditions, it is difficult and in many cases intractable to obtain analytical solutions that satisfies the governing differential or gives the extreme value to the governing functional [8]. This challenge is usually solved using another method called the numerical analysis method. This method is based on discretization of the model into smaller elements where the results are obtained by performing thousands of repetitive calculations by utilizing computers. However, it should be noted that the results obtained from the numerical method are not exact; it is an approximate solution that satisfies the equilibrium within a predefined tolerance [7].

One method of the numerical method is FEM which gives an approximate solution to boundary values for a set of partial differential equations that describes the equilibrium of the structure at hand. The general idea behind this method is first to simplify the structure into a model that represents the structural behavior correctly, thus has the appropriate boundary conditions and material/physical properties. Then, discretize it into a finite number of simplified elements where it is easier to find solutions to [7].

FEM is superior to the classical methods only for the problems involving a number of complexities that cannot be handled by classical methods without making drastic assumptions. For all regular problems, the solutions by classical methods are the best

solutions. In fact, to check the validity of the FEM programs developed, the FEM solutions are compared with the solutions by classical methods for standard problems [9].

The choice of finite element types, representation of boundary conditions, loads, and definition of the finite element mesh all play critical roles in determining how well the numerical model is able to predict the responses of the physical structure [10].

Because of finite element element's diversity and flexibility as an analysis tool, it is receiving much attention in engineering. The fast improvements in computer hardware technology and slashing of cost of computers have boosted this method, since the computer is the basic need for the application of this method. A number of popular brand of finite element analysis packages are now available commercially. Some of the popular packages are STAAD Pro, SAP2000, Abaqus and ANSYS [9].

Among this software package, SAP2000 is design oriented software program for design of bridges and buildings. It has a single user interface to model, analyze and design to get the output results using customizable window. SAP2000 has a powerful user interface to design, display and analyze any type of structure with the help of grid which can be edited as required to suit the plan of the building. This software program has a wide selection of parametric templates for different types of structures such as 3D frames, trusses, staircases, dam structures, shells and pipes which makes the modeling easy fast and is more suited for the analysis and design of such structures. The tasks such as material properties, sections, mass source, coordinate system/grids, joint constraints, joint patterns, functions (response spectrum, time history), load patterns, load cases, load combination, moving loads, pushover parameters sets are grouped under a common heading 'define' menu. The output detail of the SAP2000 gives the results in the form of shear, moment and deflection and its graphical representation [11].

2.3 Parameters Influencing the Structural Behavior

The structural parameters affecting the behavior of the reinforced concrete hypar shell can be broadly classified into five categories:

1. Geometric shape of the hypar shell

2. Properties of the supporting beams
3. Boundary conditions
4. Loading
5. Material Properties

Since the number of parameters affecting the behavior of the shell is quite large and their interaction is very complex, attempts to show their effects on the structural behavior by means of formulae would involve extensive computational work [12]. However, based on the analysis of some selected structures it is possible to show qualitatively the effects of different parameters on the behavior of a hypar shell.

2.3.1 Geometric shape

2.3.1.1 Rise to span ratio

According to membrane theory, shells with higher rise value have more reserved strength; thus, are stronger than shells with lower rise. To arrive at a more definite conclusion about the actual strength of the shell, however, the stability requirements must also be taken into consideration. Lower buckling factors were obtained when the rise to span ratio decreased and when edge beams were not used [2] & [5].

With the increase of rise to span ratio, the curvature of the surface increases. This increase in curvature reduces the bending action of the shell whereas the membrane action is increased and this eventually leads to the decrease in the central deflection [12], [13], [14], [15] & [16].

The peak tensile stress magnitudes were similar to those obtained by the membrane theory when the rise to span ratio was relatively high. However, when the rise to span ratio decreased, the magnitude of peak tensile stress was much smaller than that expected by the membrane theory. The magnitude of principal stress is inversely proportional to the rise to span ratio [5], [12] & [16].

In the case of principal compressive stress, when the rise to span ration is high and edge beams are used, an almost uniform compressive stress is observed. On the contrary, when the rise to span ratio is low and edge beams are not used; compressive stress is concentrated

at the middle (i.e., diagonal line from the crown to edge). The magnitude of principal compressive stresses was higher than predicted by the membrane theory regardless of rise to span ratio, which implies that the load is transferred to the edge through convex arch action (i.e., compressive arch action) [5], [12] & [16].

2.3.1.2 Ratio of side length (b/a)

Deflections decrease consistently as the ratio of side lengths goes between 1 and 2, the optimal form is not square. For volumetric displacement, the optimal form is a square. Taking into consideration the aesthetic point of view as constrain, the optimum value for side length ratio equal to one i.e. the shell is square, if a range is wanted to be set, a range from 1 to 2 is optimum as deflection and volumetric displacement curves are approximately flat in this range and after that the curves are steep [13] & [14].

2.3.1.3 Thickness

Deflection decreases with thickness increases due to the increase in the shell stiffness. In the other hand volumetric displacement variation increases as thickness is increased due to the increase in dead weight, with a minimum value when the thickness equal 120 mm. When taken into consideration the maximum compressive stress in shell does not exceed allowable compressive strength of concrete, and the displacements must be less than the limit set by standards, the values are safe [15].

The bending moments and the shearing forces decrease with the increase in the shell thickness that is due to the decrease in the variation of the vertical displacement. The axial force decreases with the increase in the shell thickness [17].

2.3.2 Properties of the supporting beams

2.3.2.1 Size

With increasing the cross sectional dimensions of the ridge beam, the vertical displacement at the center of the hypar shell will decrease. This behavior is due to the four ridge beams meeting at the center of the hypar shell and they will increase the hypar shell stiffness and so to decrease the vertical displacement at the same position The values of the bending moment, shearing force and axial force in the ridge beam will increases with increasing its

cross sectional dimensions. This behavior is due to the fact that the ridge beam stiffness is increased and will attract more forces [14] & [17].

With increasing the cross sectional dimensions of the edge beam, the vertical displacement at the center of the beams will decrease while it will increase near edges. This behavior is due to the increase in the edge beam rigidity by increasing its cross sectional dimensions. With increasing the cross-sectional dimensions of the edge beam, the bending moment and the axial force in the edge beam will increase which is due to the increase in the beam stiffness. The shear force increases at the center of the beam with increasing its cross sectional dimensions which is due to the increase in its stiffness [14] & [17].

2.3.2.2 Beam offset

The inverted edge beam has a higher efficiency in its structural behavior that is reflected in a smallest value of maximum deflection and volumetric displacement. By taking into consideration the aesthetic point of view as constrain, this optimum case is very good for the shell view from bottom [14].

When the beam is in a down standing position, the shear coming from the shell is transferred to the beam along its top. This eccentric force acting on the beams produces moments that add to the moments due to self-weight. In turn, this effect produces additional moments and deflections in the structure. The critical zone for this effect is the region near the crown, where the shell is almost flat and it is not able to help the beams carry their weight. For the case with the beam upstanding, the shear coming from the shell is transferred along the bottom of the member, and consequently, the moments generated are opposite to the moments induced by self-weight. The crown beams in this case are able to carry a considerable amount of the shell shear force as compressive axial force [18].

2.3.3 Boundary conditions

The displacements for fixed and hinged boundary conditions are found to be equal for hypar shell in all cases since the stiffness does not affect much by changing the boundary conditions [15].

Lateral support movement tends to affect the stability of the structure. Such movement caused a considerable increase of shell deflection, an increase of the tensile stresses, a

decrease of compressive stresses, and an intensified stress variation at the shell, which seemed to be reflective of a weakened compressive arch action [5].

2.3.4 Loading

The vertical displacement decreases at the center under the concentrated load and increases near the edges. This behavior is the result of increasing the shell rigidity, i.e. the hypar shell tries to reduce the vertical displacement [17].

Unsymmetrical loading produces considerably larger deflections and stresses than uniform loading. Partial loading on hypars produces a maximum deflection. Therefore, the linear elastic analysis adequately represents the behavior of the shell for low levels of loads. However, as the load level increases it is necessary to incorporate the effects of instability in the analysis [11].

2.3.5 Material properties

2.3.5.1 Effects of creep and shrinkage

The following are effect of creep and shrinkage of the reinforced concrete hypar [18].

- Increasing the amount of cracking in the structure, especially in the shell along the connection with the beams
- Amplifying the deformation resulting in increased the bending leading in cracking in weak support
- Pronouncing stress resultants concentrate in a region around the Crown Point, where the shell is flatter, which increase the deflections and cracking in that region.
- Amplifying the bending moments due to the shear transfer from the shell through the top portion of the beams for down standing crown beams

CHAPTER 3 MODELLING AND ANALYSIS

3.1 Selection of the Parameters

Analytical analyzing the gabled hypar reinforced concrete shell by formula involves extensive computational work since the parameters affecting its behavior is quite large and their interaction is complex. However, based on the analysis of some selected gabled hypar reinforced concrete shells it is possible to show qualitatively the effects of different parameters on the behavior of gabled hypar reinforced concrete shell.

Accordingly, the parametric studies are carried out for three categories that are major factors affecting the behavior of the hypar shell. These categories are the shell geometry, beam dimensions and material properties.

The base parameters used for the parametric analysis of gabled hypar reinforced concrete shell are stated below.

- Shell rise is 5m,
- Shell length is 20m,
- Shell width is 20m,
- Shell thickness is 0.1m,
- Beam width is 400mm,
- Beam depth is 800mm, and
- Concrete grade is C25/30.

3.1.1 Shell geometry

The major category affecting the structural performance of the gabled hypar reinforced concrete shell is the shell geometry. The parameters taken among the shell geometry for this thesis are rise to span ratio, ratio of the side (length to width ratio) and thickness.

A. Shell rise to span ratio

The first parametric study is carried out by varying rise to span ratio (h/a) as a variable making the other parameters constant. This is done by taking nineteen rise to span ratio

ratios. i.e. 0.10, 0.15, 0.20, 0.25, 0.30, 0.35, 0.40, 0.45, 0.50, 0.55, 0.60, 0.65, 0.70, 0.75, 0.80, 0.85, 0.90, 0.95 and 1.0. These ratios are obtained by varying the rise of the base shell from 1m to 10m with 0.5m interval.

B. Shell ratio of the Side

The second parametric study is carried out by varying ratio of the sides (b/a) with constant area as the other parameters constant. The dimension of the sides for this thesis are obtained by taking constant area of 400m^2 and varying the ratio of the sides with 0.25 interval as tabulated below.

Table 1. Length and width for shell ratio of the sides

Samples	Ratio	Length (m)	Width (m)
1	1.00	20.00	20.00
2	1.25	22.40	17.90
3	1.50	24.60	16.30
4	1.75	26.45	15.10
5	2.00	28.30	14.15
6	2.25	30.00	13.35
7	2.50	31.65	12.65
8	2.75	33.15	12.05
9	3.00	34.65	11.55
10	3.50	37.45	10.70
11	4.00	40.00	10.00

C. Shell thickness

The third case is analyzing the structure by varying the thickness of the shell by keeping the other parameter constant. The IS:2210-1988 recommends the shell thickness as the it shall not normally be less than 50mm if singly curved and 40mm if doubly curved [19]. Accordingly, the selected thicknesses of the shell for this thesis are 60mm, 80mm, 100mm, 120mm, 150mm, 180mm, 200mm and 250mm.

3.1.2 Beam dimensions

Since the beams along its edges support and confine the gabled hypar shell, the effects of these beams on the structural performance of the shell needs assessment. Accordingly, depth and width of the edge beam, ridge beam and tie beam are selected among the beam dimensions for this thesis. The depth of the beams are selected by checking deflection requirement for the depth to span ratio of the beam as per ES EN 1992-1-1:2015 [20] and the width of the beams are selected based on the practical limitations.

A. Depth of the edge beam

The first selected parameter under this category is varying the edge beam depth from 500mm to 1000mm with 50mm interval by taking other parameters constant.

B. Depth of the ridge beam

The second parameter to vary is depth of the ridge beam from 500mm to 1000mm with 50mm interval by taking other parameters constant.

C. Depth of the tie beam

The third case under this category is to vary depth of the tie beam from 800mm to 1200mm with 50mm interval by taking other parameters constant.

D. Width of edge beam

The fourth dimension selected is varying the width of the edge beam from 300mm to 700mm with 50mm interval by taking other parameters constant.

E. Width of the ridge beam

The fifth selected parameter under this category is varying the ridge beam width from 300mm to 700mm with 50mm interval by taking other parameters constant.

F. Width of the tie beam

The last parameter to vary is width of the tie beam from 300mm to 700mm with 50mm interval by taking other parameters constant.

3.1.3 Material properties

Even if the effect of the material property is less as the gabled hypar shell resists load mostly from the geometric feature, understanding the effect of the material property is necessary to confirm the same. Among the material properties of the structure, the concrete class is selected for this thesis. The concrete class selected for this thesis are C20/25, C25/30, C30/37, C35/45, C40/50, C45/55 and C50/60 for both the shell and the beams.

3.2 Computation of the Action on the Structure

Among the actions that act on the gabled hypar shell roof self-weight from permanent actions and imposed load on the roof from the variable action are selected for this thesis.

A. Self-weight

The self-weight of the roof is calculated as follows for analytical calculation and the program calculate the self-weight based on the properties of the material is defined in the program.

The unit weights of concrete are taken from table A.1- construction material-concrete and mortar of ES EN 1991-1-1:2015 Annex A to be 25kN/m^3 [21].

Self-weight of concrete = unit weight × thickness

=25kN/m^3 × t, m = $25t$ kN/m^2

B. Imposed Loads on Roof

According to ES EN 1991-1-1:2015 section 6.3.4 table 6.9 the roof is categorized as H and the imposed loads on the roof of this category is recommended to be 0.4kN/m^2 as per table 6.10 [21].

C. Load Combination

According to ES EN 1990:2015 sections 6.4.3.2 the general format of combination of action for persistent or transient design situation for ultimate limit stated should be [21]:

$$E_d = \gamma_{s_d} E\left\{\gamma_{g,j} G_{k,j};\ \gamma_p P;\ \gamma_{q,1} Q_{k,1};\ \gamma_{q,i} \Psi_{0,i}\ Q_{k,i}\right\}\ j \geq 1; i > 1 \quad \text{.....42}$$

where, E_d - Design value of effect of actions

γ_{s_d} - Partial factor associated with the uncertainty of action and/ or action effect model

E - Effects of actions

$\gamma_{g,j}$ - Partial factor for permanent action, which takes account of the possibility of unfavorable deviations of the action from the representative values, j

$G_{k,j}$ - Characteristics value of permanent actions, j

γ_p - Partial factors for pre-stressing actions

$\gamma_{q,1}$ - Partial factor for variable actions, which takes into account of the possibility of unfavorable deviation of the actions values from the representative values, 1

$\gamma_{q,i}$ - Partial factor for variable actions, which takes into account of the possibility of unfavorable deviation of the actions values from the representative values, i

$\Psi_{0,i}$ - Factor for combination values of variable action i

$Q_{k,i}$ - Characteristics value of the accompanying variable action i

In addition, according to ES EN 1990: 2015 table A1.2(A)-design values of action the reccomended values of partial factors for unfavorable condition are [22]:

$$\gamma_{g,j} = 1.35$$

$$\gamma_{q,1} = 1.50$$

Accordingly, the design values of the actions are:

- Self-weight: $1.35\times 25t$ kN/m^2= $33.75t$kN/m^2
- Imposed Loads on Roof: 1.5×0.4kN/m^2= 0.6kN/m^2

3.3 Verification of the Numerical Analysis

The solution of the hypar shell equation for realistic boundary conditions is complicated mathematical proposition. Following this, numerical analysis method using FEM with help of software packages is chosen because of its versatility in handling realistic boundary conditions, different structural configurations, different materials and any forms of loading with ease. Among the available the finite element software package SAP2000v20.2 is preferred for this thesis since it is familiar and it has predefined template for the hypar shell that make ease the modelling.

However, before carrying out the parametric study using the SAP2000v20.2 for the hypar shell, the result of SAP2000v20.2 shall be verified. To verify it the analytical analysis formula developed in previous chapter are used. The samples used for verification of the analysis result with their parameters are given in the following table.

Table 2. Samples with parameters for the verification of shell result

Parameters	Samples				
	1	2	3	4	5
Shell rise	3m	2m	3m	5m	3m
Shell length	20m	20m	30m	20m	40m
Shell width	20m	20m	20m	20m	20m
Shell thickness	0.10m	0.12m	0.10m	0.80m	0.12m
Beam width	400mm	400mm	500mm	400mm	750mm
Beam depth	600mm	600mm	1000mm	600mm	1500mm
Concrete grade	C25/30	C25/30	C25/30	C25/30	C25/30

3.3.1 Analytical analysis

In this part, the analytical analysis is carried out based on the formula derived on the previous chapter for above five samples.

Sample-one

i. Membrane analysis

The constant value of membrane shear force field using equation (14) is:

$$N_{xy} = -\frac{1}{2}\,hP = -\frac{1}{2}\,\frac{ab}{h}\,P = -\frac{10\times 10}{2\times 3}\times(33.75\times 0.1+0.6)$$

$$= -66.25\ {}^{kN}/_{m^2}/_{m}$$

The principal stresses associated with this internal force can be obtained from the following well-known formula:

$$t\sigma = t\left[\frac{\sigma_x+\sigma_y}{2} + \sqrt{\left(\frac{\sigma_x+\sigma_y}{2}\right)^2 + \sigma^2{}_{xy}}\right] \quad \text{.....42}$$

Which gives

$$N = t\sigma = \pm N_{xy} = \mp 66.25\ {}^{kN}/_{m^2}/_{m}$$

From which we find

$$\sigma = \frac{\mp 66.25}{0.1} = \mp 6.62\ {}^{kN}/_{m^2}$$

ii. Bending analysis

Considering that the edge beams cannot resist torsion, we may assume that the edges can rotate freely, and use Loof formula for hinged edges.

The maximum bending moment occurs at a section located at a distance y_1 from the edge, using equation (40) as,

$$Y_1 = 0.55(\frac{h}{t})^{-1/3}\, a = 0.55 \times (\frac{3}{0.1})^{-1/3} \times 10 = 1.77m$$

And the corresponding bending moment is computed using equation (41) as,

$$M_y|_{max} = +0.149Pa^2(\frac{h}{t})^{-4/3} = +0.149 \times (33.75 \times 0.1 + 0.6) \times 10^2 \times (\frac{3}{0.1})^{-4/3}$$
$$= 0.64kNm/m$$

Similarly,

For sample-two

$\tau = -116.25\ {}^{kN}/_{m^2}\big/_{m}$ and $M_y|_{max} = 1.63kNm/m$

For sample-three

$\tau = -99.38\ {}^{kN}/_{m^2}\big/_{m}$ and $M_y|_{max} = 1.43kNm/m$

For sample-four

$\tau = -33.00\ {}^{kN}/_{m^2}\big/_{m}$ and $M_y|_{max} = 0.20kNm/m$

For sample-five

$\tau = -155.00\ {}^{kN}/_{m^2}\big/_{m}$ and $M_y|_{max} = 3.79kNm/m$

3.3.2 Numerical analysis

The numerical analysis is carried out by modelling the hypar shell using SAP2000v20.2 and the response the structure is obtained from the model. Among the response of the structure obtained, the membrane shear force is tabulate in the following section for verification of the result obtained from the software. The hypar shell model created by SAP2000v20.2 is shown in the following figure.

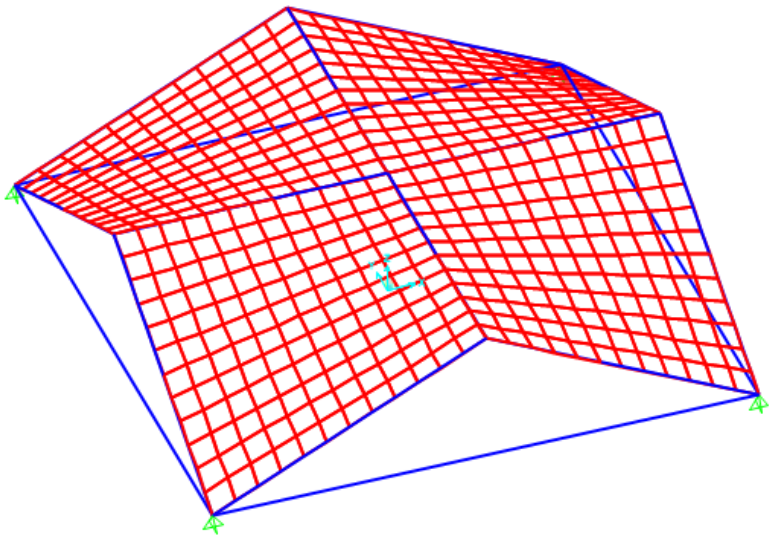

Figure 8. 3D model in SAP2000

3.3.3 Comparison of analysis result

The numerical analysis membrane shear force results for the above five samples are compared with analytical results to verify the result obtained from the software as tabulated below. As shown in the table 3 the membrane shear forces obtained from the software are practical sufficient to carry out the design of the hypar shell using SAP2000v20.2.

Table 3. Comparison of the analysis

Sample	Analytic analysis ($kN/m^2/m$)	Numerical Analysis (FEM) ($kN/m^2/m$)	Difference (%)
1	66.25	66.82	1.51
2	116.25	113.97	1.96
3	99.38	108.01	8.68
4	33.00	32.96	0.12
5	155.00	177.43	14.47

CHAPTER 4 RESULTS AND DISCUSSION

The analysis of the hypar shell is carried out for total one hundred eleven samples by modelling with SAP2000v20.2 finite element software package and the response of the structure for the actions are obtained (attached in the Appendix). The membrane shear force and displacement are selected among the response of the hypar shell. The analysis result are presented using graphs and discussion on the analysis result are stated below case by case basis.

4.1 Shell Geometry

In this part, the thesis concentrates on how change in geometry of the shell affects the structural behavior of the hypar shell. As described in the previous chapter rise to span ratio, ratio of the side and thickness of the shell were selected for the parametric study. The output of this analysis is presented for each shell for varying geometry as follows.

4.1.1 Shell rise to span ratio

In this section, the effect of shell rise to span ratio on the performance of reinforced concrete hypar shell is discussed by obtaining the variation in membrane shear force and displacement of the hypar shell.

As shown in figure 9, the membrane shear force decrease as the shell rise to span ratio increase. The increase in shell rise to span ratio from 0.10 to 1.00 decrease the membrane shear force by 66.15%. This decrease in the membrane shear force is due to the shell with higher rise value have more reserved strength than shells with lower rise. In other words, the stiffness of the shell increases with increase in rise.

The analysis result shown in figure 10 shows the displacement decrease as the shell rise to span ratio increase. The displacement is decreased by 95.68% as the shell rise to span ratio increase from 0.10 to 1.00. However, the displacement rate of decrease is decreasing as the shell rise to span is increasing and the displacement is less 2.00mm for shell rise to span ratio greater than 0.5. With the increase of rise to span ratio (RSR), the curvature of the surface increases. This increase in curvature reduces the bending action of the shell

whereas the membrane action is increased and this eventually leads to the decrease in the central deflection.

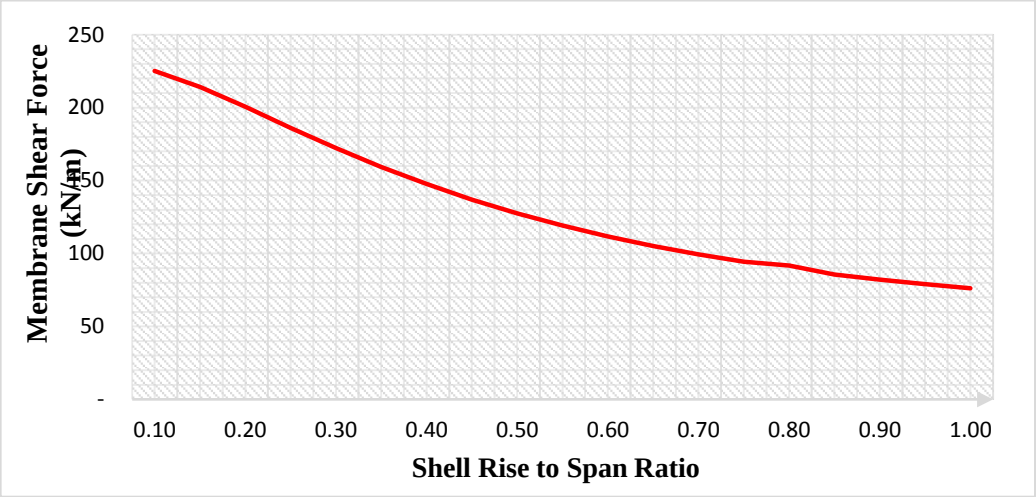

Figure 9. Membrane shear force with varying shell rise to span ratio

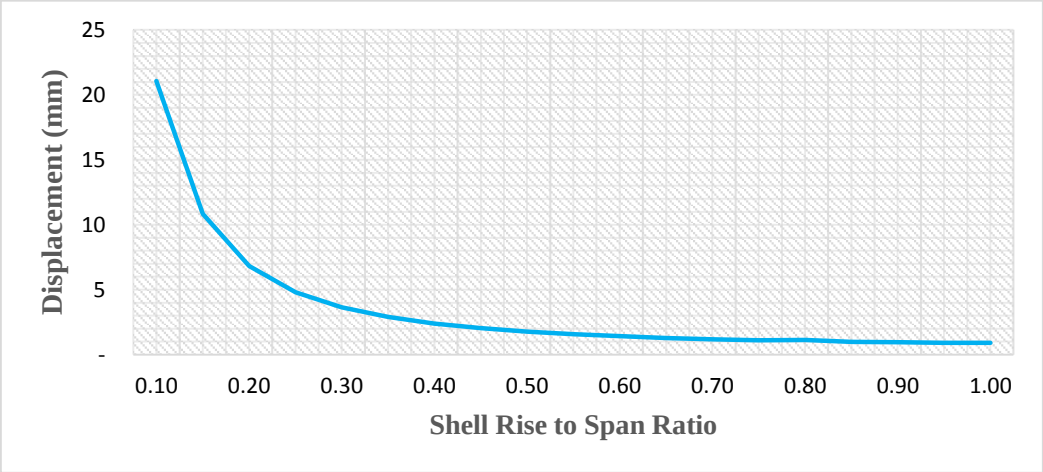

Figure 10. Displacement with varying shell rise to span ratio

4.1.2 Shell ratio of the side

The effect of shell ratio of the side on the performance of reinforced concrete hypar shell is discussed in this section based on the variation in membrane shear force and displacement. The membrane shear force increase as the shell ratio of the side increase as shown in figure 11. The increase in shell ratio of the side from 1.00 to 4.00 increase the membrane shear force by 444.11%.

As shown in figure 12, the displacement increase with increase of the shell ratio of side increase. The increase in shell ratio of the side from 1.00 to 4.00 increase the displacement by 183.54%.

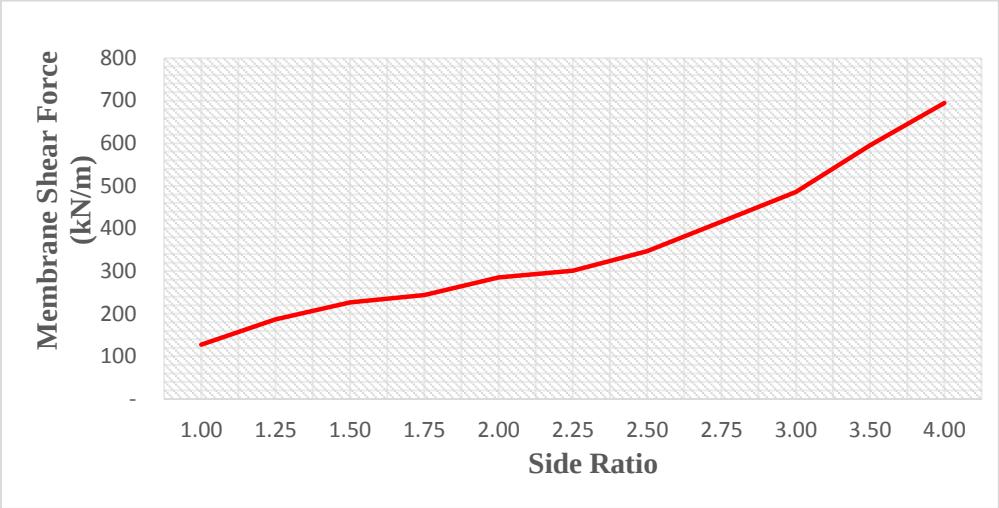

Figure 11. Membrane shear force with varying side ratio

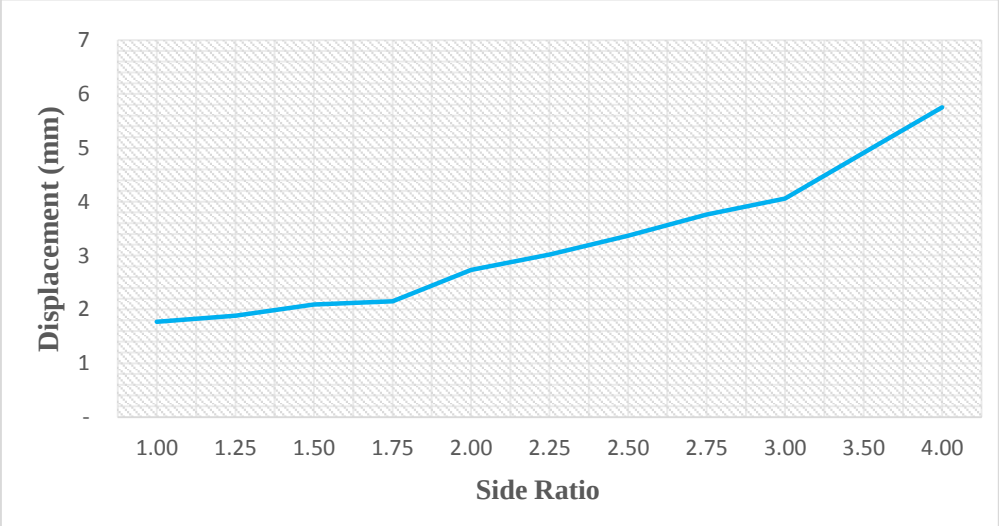

Figure 12. Displacement with varying side ratio

4.1.3 Shell thickness

In this section, the effect of shell thickness on the performance of reinforced concrete hypar shell is discussed depending on the variation in membrane shear force and displacement of the hypar shell.

The analysis result shown in figure 13 indicates the membrane shear force increase as the shell thickness increase. The membrane shear force increased by 460.93% as the shell

thickness increase from 0.06m to 0.25. The membrane shear forces decreases with the increase in the shell thickness due to increases shell stiffness with the increase in the shell thickness. However, as the shell thickness increase the self-weight of the shell increase significantly which result in increase of membrane shear force.

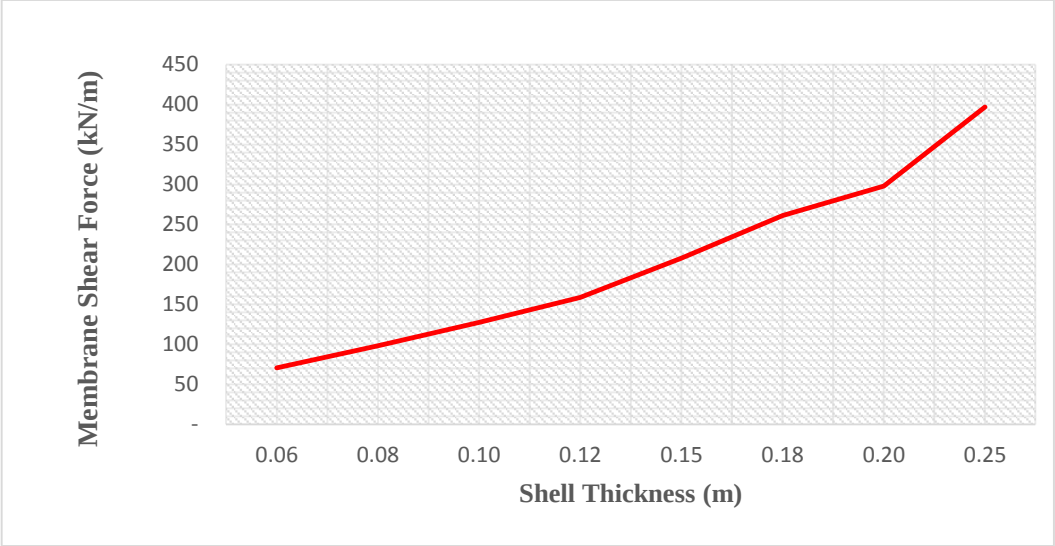

Figure 13. Membrane shear force with varying shell thickness

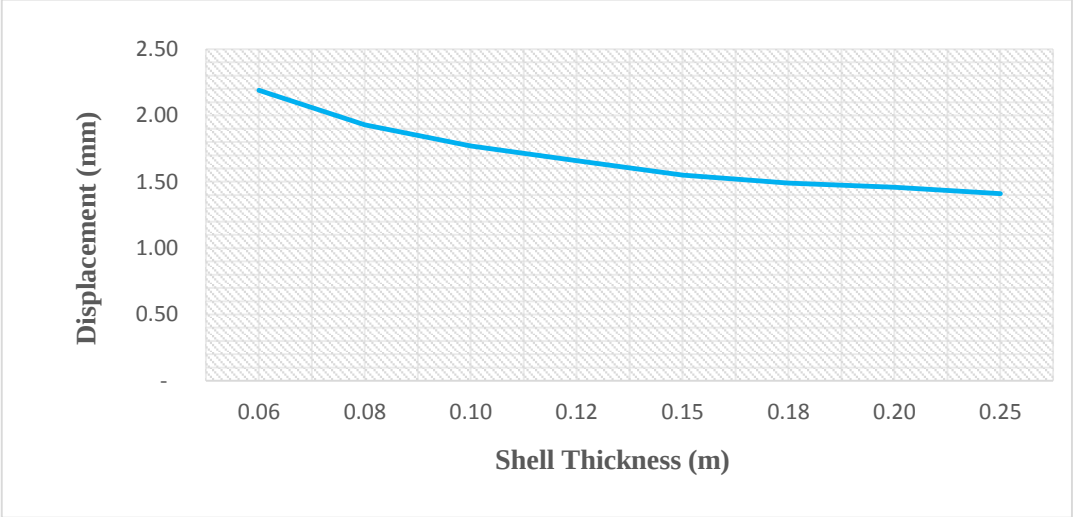

Figure 14. Displacement with varying shell thickness

As shown in figure 14, the displacement decrease as the shell thickness increase. The increase in shell thickness from 0.06m to 0.25m decrease the displacement by 35.62%. However, the displacement rate of decrease is decreasing as the shell thickness increasing. The decrease in the displacement results due to the increase in the shell stiffness as the shell thickness increase.

4.2 Beam Dimensions

In this part, the thesis concentrates on how beam dimensions affects the structural behavior of the hypar shell. As described in the previous chapter depth and width of edge beam, ridge beam and tie beam were selected for the parametric study. The output of this analysis is presented graphical case by case below.

4.2.1 Depth of the edge beam

In this section, the effect of depth of the edge beam on the performance of reinforced concrete hypar shell discussed depending on the variation in membrane shear force and displacement of the hypar shell.

The analysis result shown in figure 15 indicates the membrane shear force decrease as the edge beam depth increase. The membrane shear force decreased by 50.91% as the edge beam depth increase from 0.50m to 1.00m. The rate of decrease of the membrane shear force is decreasing as the depth of the edge increase. Since the stiffness of the shell increase as the edge beam depth increase, the membrane shear force decrease with increase in the depth of edge beam.

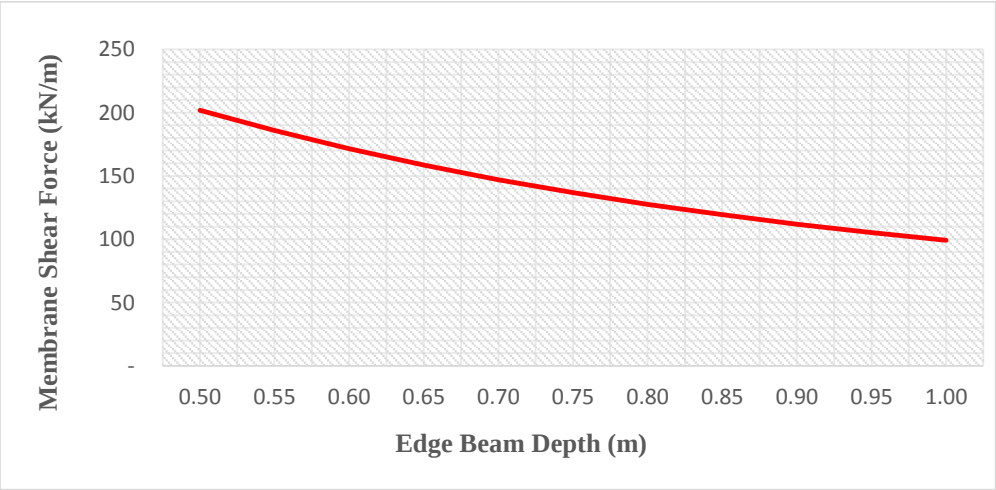

Figure 15. Membrane shear force with varying edge beam depth

As shown in figure 16, the displacement decrease as the edge beam depth increase. The increase in edge beam depth from 0.50m to 1.00m decrease the displacement by 10.94%. With increasing the depth of the edge beam, the displacement decrease due to the increase in the edge beam rigidity by increasing its depth.

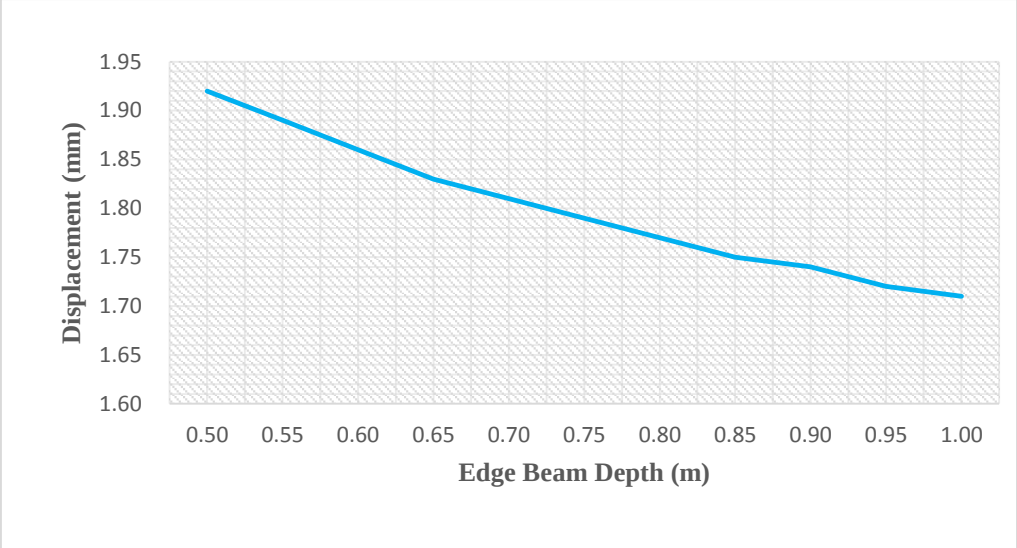

Figure 16. Displacement with varying edge beam depth

4.2.2 Depth of the ridge beam

The effect of ridge beam depth on the performance of reinforced concrete hypar shell is discussed in this section based on the variation in membrane shear force and displacement.

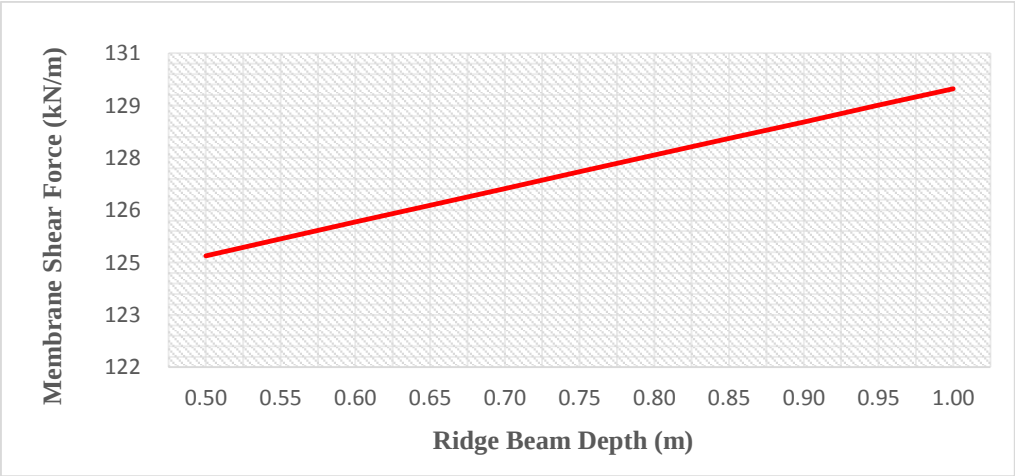

Figure 17. Membrane shear force with varying ridge beam depth

The membrane shear force increase with the ridge beam depth increase as shown in figure 17. The increase in ridge beam depth from 0.50m to 1.00m increase the membrane shear force by 3.84%. The values of the membrane shear force decreases with increasing ridge beam depth due to the increase in stiffness as its depth increase. However, the increase the depth of the ridge beam increase in the self-weight of the structure that result in increase in the membrane shear force.

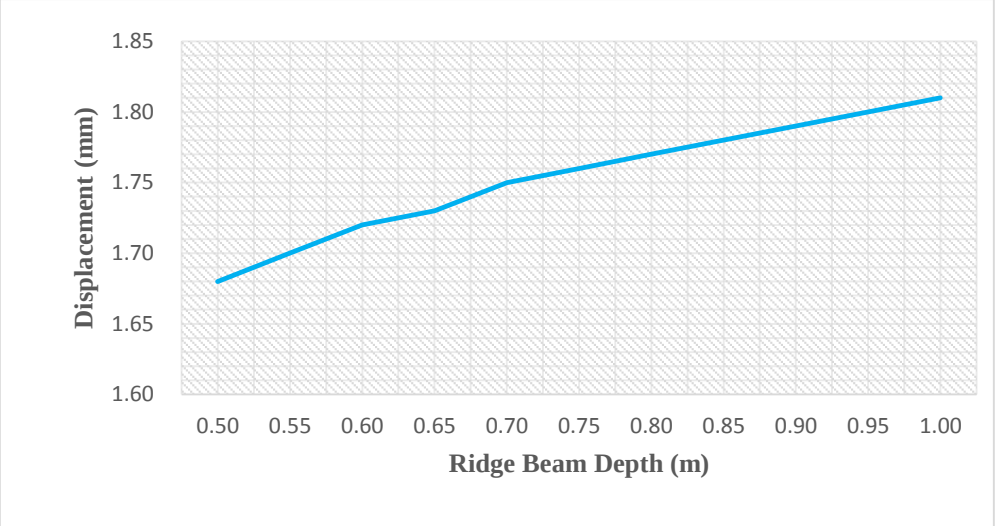

Figure 18. Displacement with varying ridge beam depth

As shown in figure 18, the displacement increase with the ridge beam depth increase. The increase in ridge beam depth from 0.50 to 1.00 increase the displacement by 7.74%. With increasing the depth of the ridge beam the displacement the shell decrease due to increase the shell stiffness. However, the increase the depth of the ridge beam increase in the self-weight of the structure that result in increase in the displacement.

4.2.3 Depth of the tie beam

In this section, the effect of depth of the tie beam on the performance of reinforced concrete hypar shell discussed depending on the variation in membrane shear force and displacement of the hypar shell. Tie beams are used to restrain excessive lateral movements.

The analysis result shown in figure 19 indicates the membrane shear force is constant as the tie beam depth increase. As shown in figure 20, the displacement is constant the tie beam depth increase. The minimum depth provided for deflection requirement in tie beam large as the span of the beam is large. In general, the minimum depth of the tie beam provided for deflection of the beam is sufficient restrict the lateral movement of the shell and the effect of the depth of the tie beam is not recognized by increasing the its depth above the requirement for deflection.

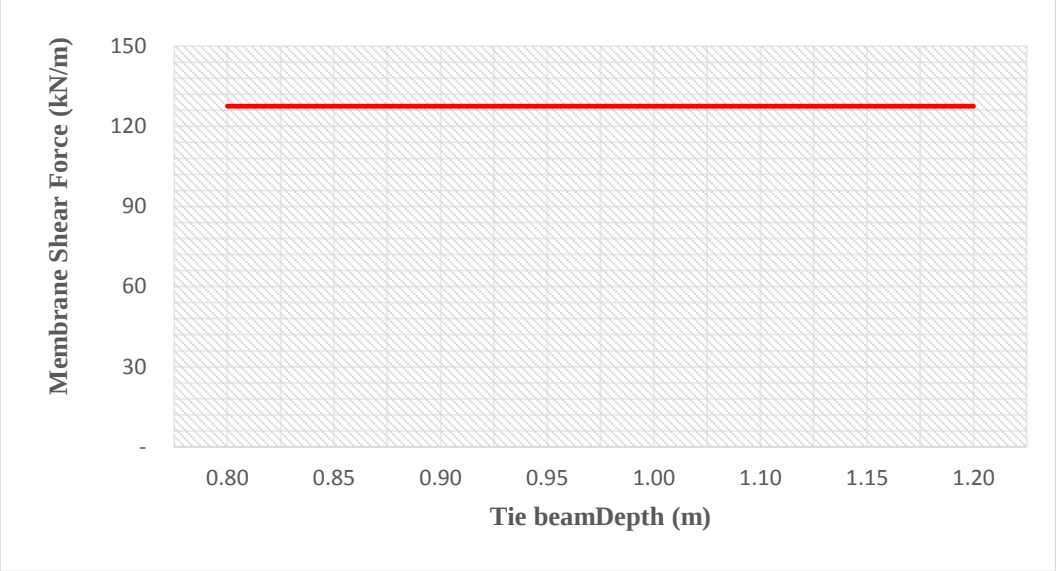

Figure 19. Membrane shear force with varying tie beam depth

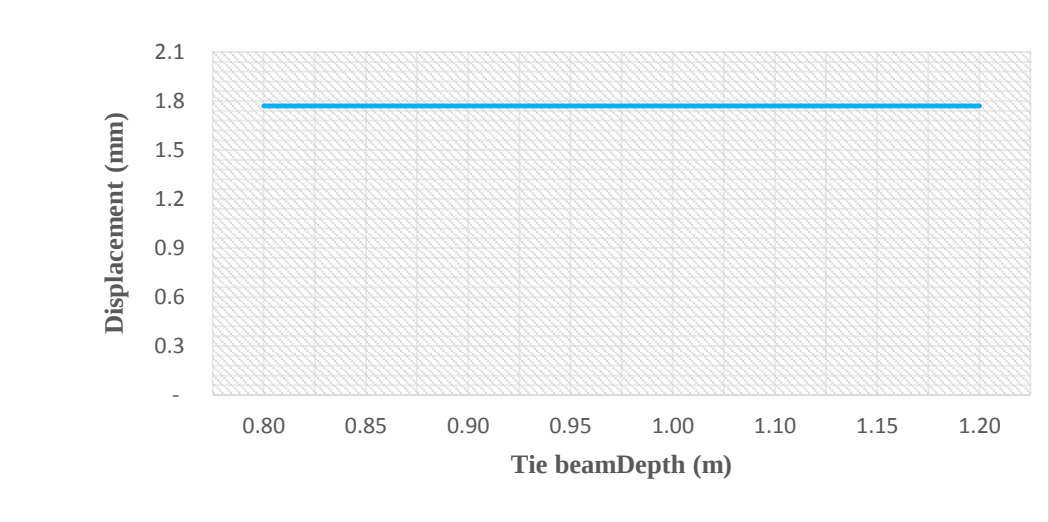

Figure 20. Displacement with varying the tie beam depth

4.2.4 Width of edge beam

The effect of edge beam width on the performance of reinforced concrete hypar shell is discussed in this section based on the variation in membrane shear force and displacement.

The membrane shear force decrease with the edge beam width increase as shown in figure 21. The increase in ridge beam depth from 0.30m to 0.70m decrease the membrane shear force by 59.13%. The rate of decrease of the membrane shear force is decreasing as the

edge beam width increase. The membrane shear force increases with increasing the edge beam width due to the increase in the shell stiffness.

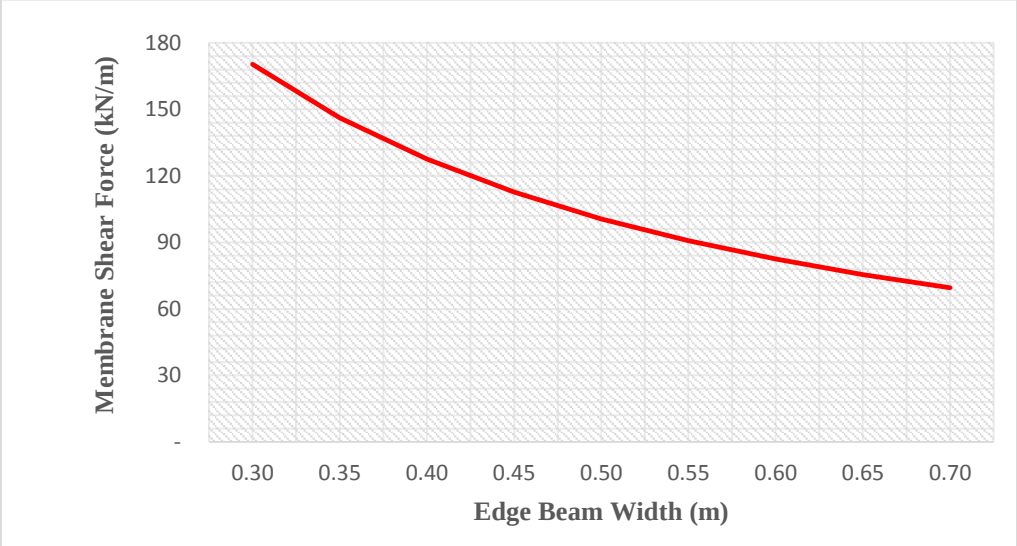

Figure 21. Membrane shear force with varying edge beam width

As shown in figure 22, the displacement decrease with the edge beam width increase. The increase in edge beam width from 0.30 to 0.70 decrease the displacement by 13.83%. With increasing the width of the edge beam the displacement decrease due to the increase in the rigidity of the structure by increasing its width.

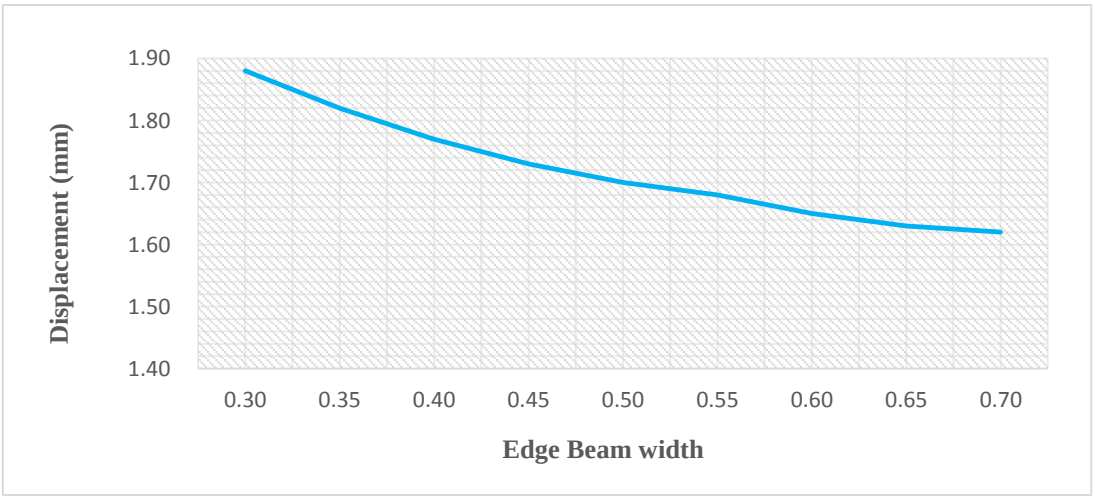

Figure 22. Displacement with varying edge beam width

4.2.5 Width of the ridge beam

In this section, the effect of ridge beam width on the performance of reinforced concrete hypar shell discussed depending on the variation in membrane shear force and displacement of the shell.

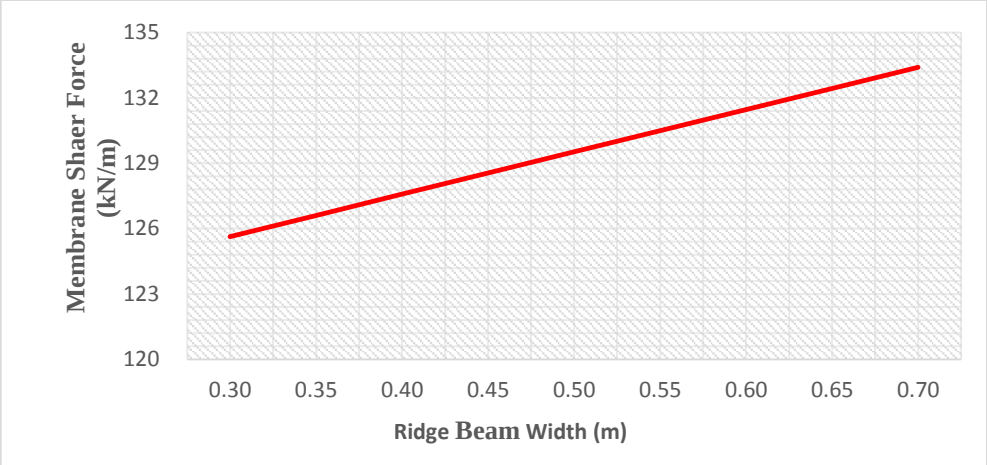

Figure 23. Membrane shear force with varying ridge beam width

The analysis result shown in figure 23 indicates the membrane shear force increase as the ridge beam width increase. The membrane shear force increased by 6.18% as the ridge beam width increase from 0.30m to 0.70m. The values of the membrane shear force decreases with increasing ridge beam width due to the increase in stiffness as its width increase. However, the increase the width of the ridge beam increase in the self-weight of the structure that result in the membrane shear force increase.

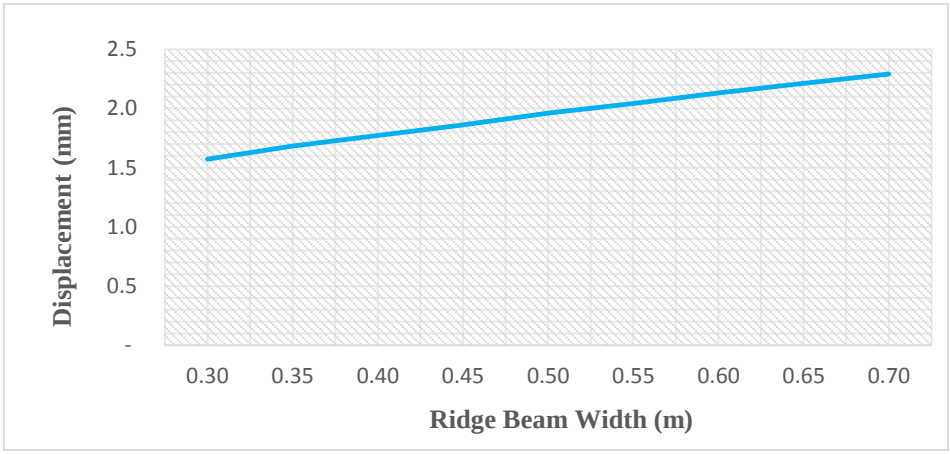

Figure 24. Displacement with varying ridge beam width

As shown in figure 24, the displacement increase as the ridge beam width increase. The increase in edge beam depth from 0.30m to 0.70m increase the displacement by 45.86%.

With increasing the width of the ridge beam the displacement of shell decrease due to increase the shell stiffness. However, the increase the width of the ridge beam increase in the self-weight of the structure that result in increase in the displacement.

4.2.6 Width of the tie beam

The effect of tie beam width on the performance of reinforced concrete hypar shell is discussed in this section based on the variation in membrane shear force and displacement.

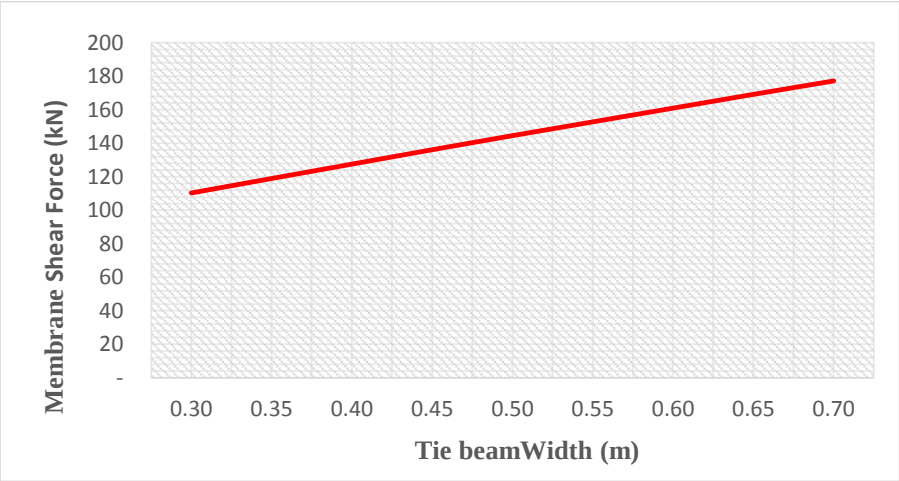

Figure 25. Membrane shear force with varying tie beam width

The membrane shear force increase with the tie beam width increase as shown in figure 25. The increase in ridge beam depth from 0.30m to 0.70m increase the membrane shear force by 60.73%. The rate of increase of the membrane shear force is decreasing as the tie beam width increase.

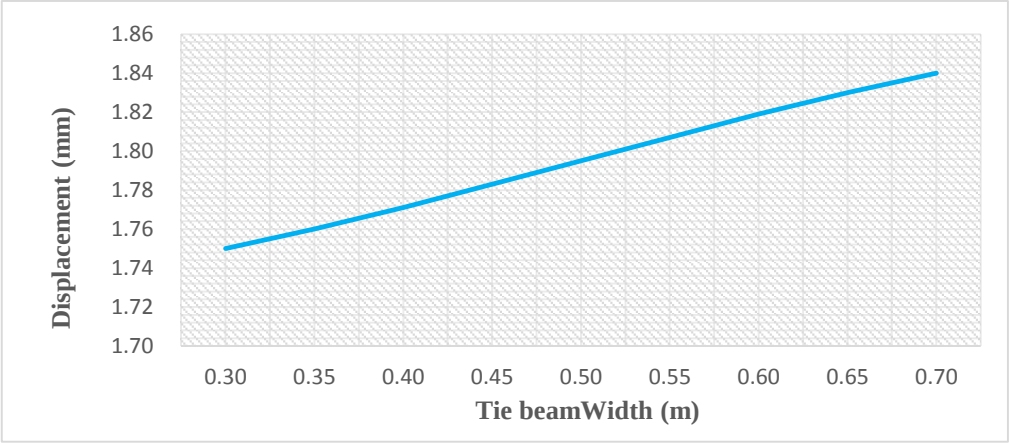

Figure 26. Displacement with varying tie beam width

As shown in figure 26, the displacement increase with the tie beam width increase. The increase in tie beam width from 0.30 to 0.70 increase the displacement 54.35%.

4.3 Material Properties

In this part, the thesis concentrates on how material property affects the structural behavior of the hypar shell. As described in the previous chapter concrete class is selected for the parametric study. The output of this analysis is presented graphical case by case below.

4.3.1 Shell concrete class

In this section, the effect of shell concrete class on the performance of reinforced concrete hypar shell discussed depending on the variation in membrane shear force and displacement of the shell.

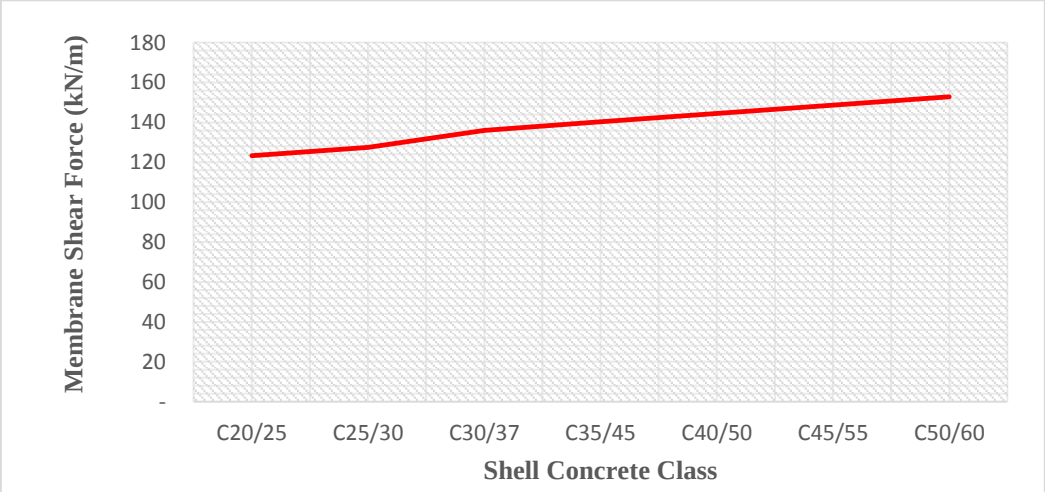

Figure 27. Membrane shear force with varying shell concrete class

The analysis result shown in figure 27 indicates the membrane shear force increase as the shell concrete class increase. The membrane shear force increased by 23.98% as the shell concrete class increase from C20/25 to C50/60.

As shown in figure 28, the displacement decrease as the shell concrete class increase. The increase in shell concrete class from C20/25 to C50/60 decrease the displacement by 11.11%.

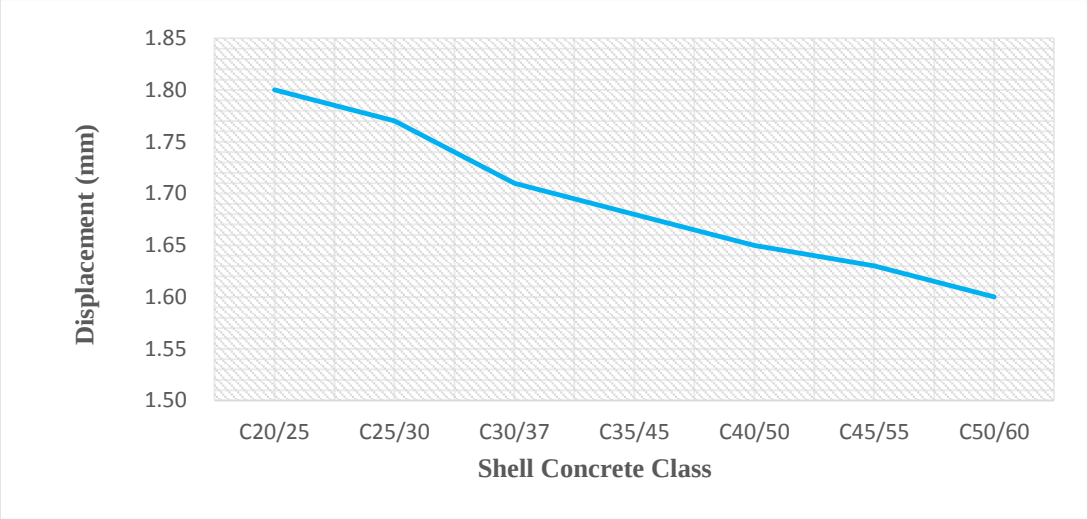

Figure 28. Displacement with varying shell concrete class

4.3.2 Edge beam concrete class

The effect of edge beam concrete class on the performance of reinforced concrete hypar shell is discussed in this section based on the variation in membrane shear force and displacement.

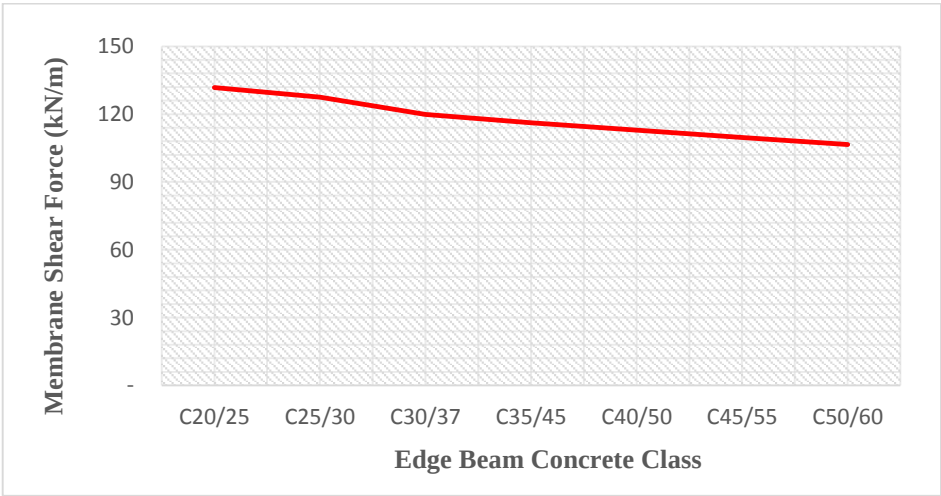

Figure 29. Membrane shear force with varying edge beam concrete class

The membrane shear force decrease with the edge beam concrete class increase as shown in figure 29. The increase in edge beam concrete class from C20/25 to C50/60 decrease the membrane shear force by 19.13%.

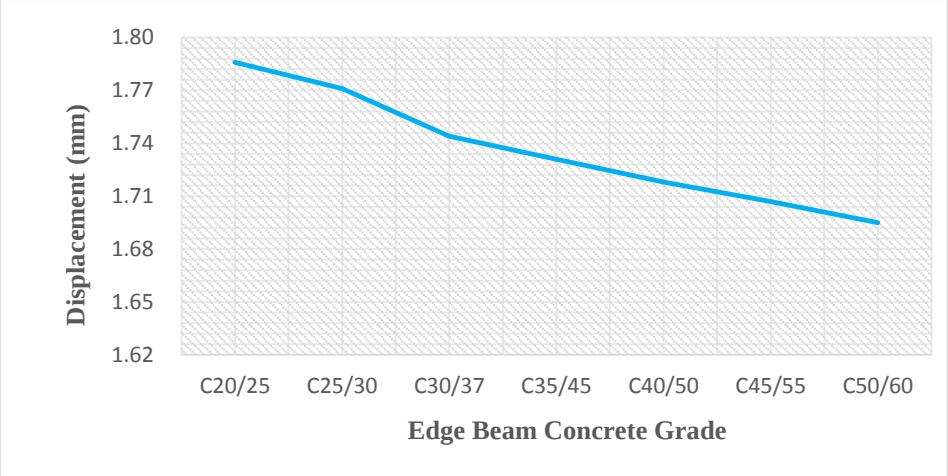

Figure 30. Displacement with varying edge beam concrete class

As shown in figure 30, the displacement decrease with the edge beam concrete class increase. The increase in edge beam concrete class from C20/25 to C50/60 decrease the displacement 5.10%.

4.3.3 Ridge beam concrete class

In this section, the effect of ridge beam concrete class on the performance of reinforced concrete hypar shell is discussed depending on the variation in membrane shear force and displacement of the shell.

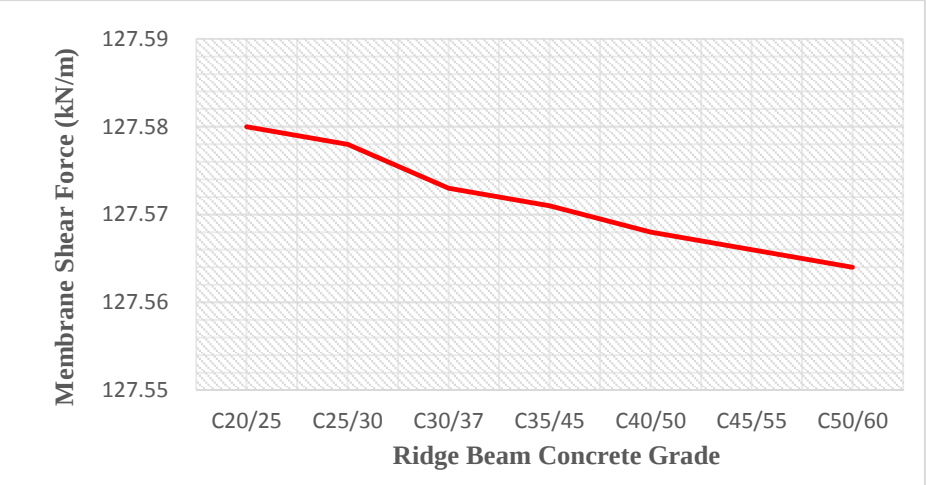

Figure 31. Membrane shear force with varying ridge beam concrete class

The analysis result shown in figure 31 indicates the membrane shear force decrease as the ridge beam concrete class increase. The membrane shear force decreased by 0.01% as the ridge beam concrete class increase from C20/25 to C50/60.

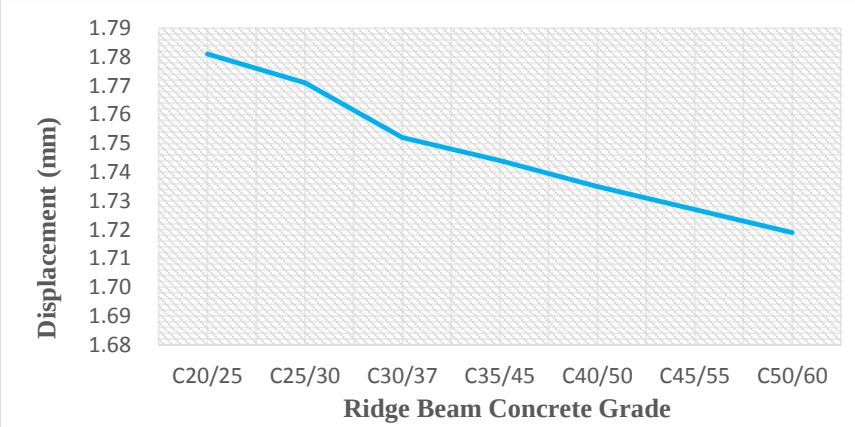

Figure 32. Displacement with varying ridge beam concrete class

As shown in figure 32, the displacement decrease as the ridge beam concrete class increase. The increase in ridge beam concrete class from C20/25 to C50/60 decrease the displacement by 3.84%.

4.3.4 Tie beam Concrete Class

The effect of tie beam concrete class on the performance of reinforced concrete hypar shell is discussed in this section based on the variation in membrane shear force and displacement.

The membrane shear force decrease with the tie beam concrete class increase as shown in figure 33. The increase in tie beam concrete class from C20/25 to C50/60 decrease the membrane shear force by 0.85%.

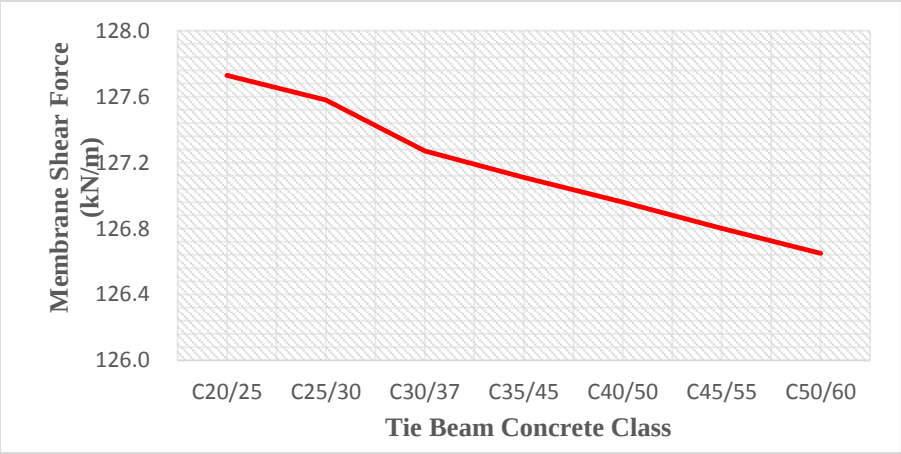

Figure 33. Membrane shear force with varying tie beam concrete class

As shown in figure 34, the displacement is constant with the tie beam concrete class increase.

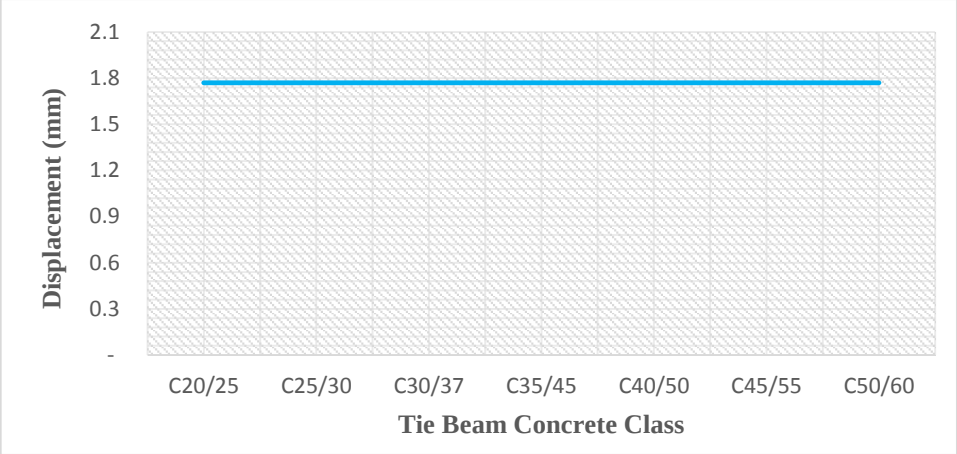

Figure 34. Displacement with varying tie beam concrete class

CHAPTER 5 CONCLUSIONS AND RECOMMENDATIONS

5.1 Conclusion

The parametric study of the gabled hypar shell is carried out using the finite element software package SAP2000v20.2 in this thesis. The parameters selected for this study are shell rise to span ratio, shell sides ratio, thickness of the shell among the shell geometry, width and depth of the edge, ridge and tie beam from the beam dimension, and concrete class among the material properties for both the shell and beams. The membrane shear force and displacement in the shell was selected from the response of the structure.

Based on the analysis result the following conclusions are drawn.

- With the increase of the shell rise to span ratio both membrane shear force and displacement are decreased
- Both membrane shear force and displacement are increased as the shell ratio of the side increase
- As the shell thickness increase the membrane shear force is increased and the displacement is decreased
- With the edge beam depth increase both membrane shear force and displacement are decreased
- Both membrane shear force and displacement are increased with the ridge beam depth increase
- As the tie beam depth increase both membrane shear force and displacement are constant
- With the edge beam width increase both membrane shear force and displacement are decreased
- Both membrane shear force and displacement are increased as the ridge beam width increase
- As the tie beam width increase both membrane shear force and displacement are increased
- The membrane shear force is increased and the displacement is decreased with the shell concrete class increase

- Both membrane shear force and displacement are decreased as edge beam concrete class increase
- With the ridge beam concrete class increase membrane shear force is slightly decreased and displacement is decreased
- As the tie beam concrete class increase the membrane shear force is slightly decreased and the displacement is constant

The major cause of the shell response variation (membrane shear force and displacement for this thesis) variation in the shell stiffness and self-weight.

5.2 Recommendations

The structural efficiency of the reinforced concrete gabled hypar shell structure increased by varation of the major parameters with the following sequence.

- decrease the shell thickness
- decrease the shell ratio of the side
- increase the shell rise to span ratio
- decrease the tie beam width
- increase the edge beam width
- increase the edge beam depth
- increase the shell concrete class
- increase the edge beam concrete class

As the parameters are listed above in sequential order, the best way to increase structural performance of the reinforced concrete gabled hypar shell is varying the geometry of the shell.

The following are recommended thesis areas to understand more about the structural performance of the reinforced concrete gabled hypar shell.

- Stability analysis of the structure supported with the parametric study of the shell
- Dynamic analysis of the structure supported with the parametric study of the shell
- The effect shrinkage and creep of the reinforced concrete

REFERENCES

[1] Varghese, P. (2010) Design of reinforced concrete shells and folded plates. New Delhi: PHI Learning Private United.

[2] Farshad, M. (1992) Design and analysis of shell structures. Switzerland: Kluwer Academic Publishers.

[3] Kadam, S., Gandhe, R. and Tupe, H. (2019) Advanced modeling and analysis of plate and inverted umbrella roof shell using ANSYS. International Journal of Science and Research. 8(2), pp.538-542

[4] Shifferaw, T. (2015) Analysis and design of shell structure. Addis Ababa: unpublished.

[5] Rha, S., Kim, N. and Yu, E. (2015) Behavior of gabled hyperbolic paraboloid shells. Journal of Asian Architecture and Building Engineering. 14(1), pp.159-166

[6] Billington, P. (1990) Thin shell concrete structure. 2nd ed. New York: McGraw-Hill Publishing Company.

[7] Ghebreselasie, M. and Situ, Y. (2015) Structural analysis of thin concrete shells. Norway, unpublished

[8] Varghese, B., Saju, A. and John, S. (2014) Finite element analysis of arch dam. International Journal of Research in Engineering and Technology. 3(7), pp.180-193

[9] Bhavikatti, S. (2005) Finite element analysis. New Delhi: New Age International Publishers.

[10] Nasir, M. (2002) Axisymmetric shell structures for multi-use. Australia: unpublished

[11] Lallotra, B. and Singhal, D. (2017) A comparative study of structural analysis and design software - STAAD Pro, SAP-2000 & ETABS software: state of the art report. International Journal of Engineering and Technology. 9(2), pp.1030-1043

[12] Peter, G., Banavalkar, P. and Parker, J. (1971) The analysis and behavior of thin-steel hyperbolic paraboloid shells. Center for Cold-Formed Steel Structures Library. 19

[13] Draper, P., Maria, E., Garlock, M. and Billington, P. (2008) Optimization of concrete hyperbolic paraboloid umbrella shells. Proceedings of the 6th International Conference on Computation of Shell and Spatial Structures.

[14] Othman, H., Tayel, M. and Marzouk, H (2014) Optimization of UHP-FRC inverted umbrella shell structures, 4th International Structural Specialty Conference. 70

[15] Sachin, V. and Suresh, R. (2018) A study on behavior of cylindrical and hyperbolic paraboloid type of shell roofs for fixed and hinged boundary conditions. International Journal of Engineering and Technology. 7, pp. 829-834

[16] Garhwal, A., Kaushik, Y., Singh, M. and Divya, (2018), Finite element analysis of hyperbolic paraboloid composite shells for static analysis under uniform pressure. Proceedings of the International Conference on Modern Research in Aerospace Engineering. pp. 189-201

[17] Aziz, J., Al-Azzawi, A. and Al-Ani, A. (2011) Finite element elastic analysis of hypar shells on winkler foundation. Journal of the Serbian Society for Computational Mechanics. 5(1), pp. 1-18

[18] Gallegos-Cazares, S. and Schnobrich, C. (1988) Effects of creep and shrinkage on the behavior of reinforced concrete gable roof hyperbolic-paraboloids. Civil Engineering Studies Structural Research Series. 543

[19] Indian Standard (1992) Criteria for design of reinforced concrete shell structures and folded plates: IS: 2210-1988. New Delhi: Bureau of Indian Standards

[20] Ethiopian Standard-Based on Euro Norms (2015) Design of Concrete Structure: Part1-1: General rules and rules for buildings: ES EN 1992-1-1:2015. Addis Ababa: Ministry of Construction

[21] Ethiopian Standard-Based on Euro Norms (2015) Action on Structures: Part 1-1: General Actions-Densities, Self-Weight, Imposed Loads for buildings: ES EN 1991-1-1:2015. Addis Ababa: Ministry of Construction

[22] Ethiopian Standard-Based on Euro Norms (2015) Basis of Structural Design: ES EN 1990:2015. Addis Ababa: Ministry of Construction

APPENDIX A SAMPLES AND ANALYSIS RESULT

Samples	Shell Rise (m)	Shell Length (m)	Shell width (m)	Shell thickness (m)	Edge Beam depth (m)	Edge beam width (m)	Ridge Beam depth (m)	Ridge beam width (m)	Tie Beam Depth (m)	Tie Beam Width (m)	Shell Concrete Grade	Edge beam Concrete Grade	Ridge beam Concrete Grade	Tie beam Concrete Grade	Membrane Shear Force (kN/m)	Displacement (mm)
1	1.00	20.00	20.00	0.10	0.80	0.40	0.80	0.40	0.80	0.40	C25/30	C25/30	C25/30	C25/30	225.18	21.07
2	1.50	20.00	20.00	0.10	0.80	0.40	0.80	0.40	0.80	0.40	C25/30	C25/30	C25/30	C25/30	214.27	10.84
3	2.00	20.00	20.00	0.10	0.80	0.40	0.80	0.40	0.80	0.40	C25/30	C25/30	C25/30	C25/30	200.48	6.83
4	2.50	20.00	20.00	0.10	0.80	0.40	0.80	0.40	0.80	0.40	C25/30	C25/30	C25/30	C25/30	186.14	4.81
5	3.00	20.00	20.00	0.10	0.80	0.40	0.80	0.40	0.80	0.40	C25/30	C25/30	C25/30	C25/30	172.29	3.64
6	3.50	20.00	20.00	0.10	0.80	0.40	0.80	0.40	0.80	0.40	C25/30	C25/30	C25/30	C25/30	159.38	2.90
7	4.00	20.00	20.00	0.10	0.80	0.40	0.80	0.40	0.80	0.40	C25/30	C25/30	C25/30	C25/30	147.62	2.39
8	4.50	20.00	20.00	0.10	0.80	0.40	0.80	0.40	0.80	0.40	C25/30	C25/30	C25/30	C25/30	137.03	2.04
9	5.00	20.00	20.00	0.10	0.80	0.40	0.80	0.40	0.80	0.40	C25/30	C25/30	C25/30	C25/30	127.58	1.77
10	5.50	20.00	20.00	0.10	0.80	0.40	0.80	0.40	0.80	0.40	C25/30	C25/30	C25/30	C25/30	119.18	1.57
11	6.00	20.00	20.00	0.10	0.80	0.40	0.80	0.40	0.80	0.40	C25/30	C25/30	C25/30	C25/30	111.74	1.42
12	6.50	20.00	20.00	0.10	0.80	0.40	0.80	0.40	0.80	0.40	C25/30	C25/30	C25/30	C25/30	105.16	1.29
13	7.00	20.00	20.00	0.10	0.80	0.40	0.80	0.40	0.80	0.40	C25/30	C25/30	C25/30	C25/30	99.35	1.19
14	7.50	20.00	20.00	0.10	0.80	0.40	0.80	0.40	0.80	0.40	C25/30	C25/30	C25/30	C25/30	94.32	1.11
15	8.00	20.00	20.00	0.10	0.80	0.40	0.80	0.40	0.80	0.40	C25/30	C25/30	C25/30	C25/30	91.66	1.13
16	8.50	20.00	20.00	0.10	0.80	0.40	0.80	0.40	0.80	0.40	C25/30	C25/30	C25/30	C25/30	85.68	0.99
17	9.00	20.00	20.00	0.10	0.80	0.40	0.80	0.40	0.80	0.40	C25/30	C25/30	C25/30	C25/30	82.14	0.95

18	9.50	20.00	20.00	0.10	0.80	0.40	0.80	0.40	0.80	0.40	C25/30	C25/30	C25/30	C25/30	79.00	0.91
19	10.0	20.00	20.00	0.10	0.80	0.40	0.80	0.40	0.80	0.40	C25/30	C25/30	C25/30	C25/30	76.23	0.91
20	5.00	22.40	17.90	0.10	0.80	0.40	0.80	0.40	0.80	0.40	C25/30	C25/30	C25/30	C25/30	186.71	1.88
21	5.00	24.60	16.30	0.10	0.80	0.40	0.80	0.40	0.80	0.40	C25/30	C25/30	C25/30	C25/30	227.88	2.10
22	5.00	26.45	15.10	0.10	0.80	0.40	0.80	0.40	0.80	0.40	C25/30	C25/30	C25/30	C25/30	244.07	2.15
23	5.00	28.30	14.15	0.10	0.80	0.40	0.80	0.40	0.80	0.40	C25/30	C25/30	C25/30	C25/30	284.87	2.73
24	5.00	30.00	13.35	0.10	0.80	0.40	0.80	0.40	0.80	0.40	C25/30	C25/30	C25/30	C25/30	301.29	3.02
25	5.00	31.65	12.65	0.10	0.80	0.40	0.80	0.40	0.80	0.40	C25/30	C25/30	C25/30	C25/30	346.86	3.37
26	5.00	33.15	12.05	0.10	0.80	0.40	0.80	0.40	0.80	0.40	C25/30	C25/30	C25/30	C25/30	416.16	3.76
27	5.00	34.65	11.55	0.10	0.80	0.40	0.80	0.40	0.80	0.40	C25/30	C25/30	C25/30	C25/30	485.56	4.06
28	5.00	37.45	10.70	0.10	0.80	0.40	0.80	0.40	0.80	0.40	C25/30	C25/30	C25/30	C25/30	595.65	4.91
29	5.00	40.00	10.00	0.10	0.80	0.40	0.80	0.40	0.80	0.40	C25/30	C25/30	C25/30	C25/30	694.17	5.75
30	5.00	20.00	20.00	0.06	0.80	0.40	0.80	0.40	0.80	0.40	C25/30	C25/30	C25/30	C25/30	70.74	2.19
31	5.00	20.00	20.00	0.08	0.80	0.40	0.80	0.40	0.80	0.40	C25/30	C25/30	C25/30	C25/30	98.28	1.93
32	5.00	20.00	20.00	0.12	0.80	0.40	0.80	0.40	0.80	0.40	C25/30	C25/30	C25/30	C25/30	158.57	1.66
33	5.00	20.00	20.00	0.15	0.80	0.40	0.80	0.40	0.80	0.40	C25/30	C25/30	C25/30	C25/30	208.11	1.55
34	5.00	20.00	20.00	0.18	0.80	0.40	0.80	0.40	0.80	0.40	C25/30	C25/30	C25/30	C25/30	261.11	1.49
35	5.00	20.00	20.00	0.20	0.80	0.40	0.80	0.40	0.80	0.40	C25/30	C25/30	C25/30	C25/30	298.23	1.46
36	5.00	20.00	20.00	0.25	0.80	0.40	0.80	0.40	0.80	0.40	C25/30	C25/30	C25/30	C25/30	396.80	1.41
37	5.00	20.00	20.00	0.10	0.50	0.40	0.80	0.40	0.80	0.40	C25/31	C25/31	C25/31	C25/31	201.90	1.92
38	5.00	20.00	20.00	0.10	0.55	0.40	0.80	0.40	0.80	0.40	C25/30	C25/30	C25/30	C25/30	185.84	1.89
39	5.00	20.00	20.00	0.10	0.60	0.40	0.80	0.40	0.80	0.40	C25/30	C25/30	C25/30	C25/30	171.44	1.86
40	5.00	20.00	20.00	0.10	0.65	0.40	0.80	0.40	0.80	0.40	C25/30	C25/30	C25/30	C25/30	158.56	1.83
41	5.00	20.00	20.00	0.10	0.70	0.40	0.80	0.40	0.80	0.40	C25/30	C25/30	C25/30	C25/30	147.06	1.81

42	5.00	20.00	20.00	0.10	0.75	0.40	0.80	0.40	0.80	0.40	C25/30	C25/30	C25/30	C25/30	136.78	1.79
43	5.00	20.00	20.00	0.10	0.85	0.40	0.80	0.40	0.80	0.40	C25/30	C25/30	C25/30	C25/30	119.32	1.75
44	5.00	20.00	20.00	0.10	0.90	0.40	0.80	0.40	0.80	0.40	C25/30	C25/30	C25/30	C25/30	111.88	1.74
45	5.00	20.00	20.00	0.10	0.95	0.40	0.80	0.40	0.80	0.40	C25/30	C25/30	C25/30	C25/30	105.17	1.72
46	5.00	20.00	20.00	0.10	1.00	0.40	0.80	0.40	0.80	0.40	C25/30	C25/30	C25/30	C25/30	99.11	1.71
47	5.00	20.00	20.00	0.10	0.80	0.40	0.50	0.40	0.80	0.40	C25/30	C25/30	C25/30	C25/30	124.69	1.68
48	5.00	20.00	20.00	0.10	0.80	0.40	0.55	0.40	0.80	0.40	C25/30	C25/30	C25/30	C25/30	125.18	1.70
49	5.00	20.00	20.00	0.10	0.80	0.40	0.60	0.40	0.80	0.40	C25/30	C25/30	C25/30	C25/30	125.66	1.72
50	5.00	20.00	20.00	0.10	0.80	0.40	0.65	0.40	0.80	0.40	C25/30	C25/30	C25/30	C25/30	126.14	1.73
51	5.00	20.00	20.00	0.10	0.80	0.40	0.70	0.40	0.80	0.40	C25/30	C25/30	C25/30	C25/30	126.62	1.75
52	5.00	20.00	20.00	0.10	0.80	0.40	0.75	0.40	0.80	0.40	C25/30	C25/30	C25/30	C25/30	127.62	1.76
53	5.00	20.00	20.00	0.10	0.80	0.40	0.85	0.40	0.80	0.40	C25/30	C25/30	C25/30	C25/30	128.06	1.78
54	5.00	20.00	20.00	0.10	0.80	0.40	0.90	0.40	0.80	0.40	C25/30	C25/30	C25/30	C25/30	128.53	1.79
55	5.00	20.00	20.00	0.10	0.80	0.40	0.95	0.40	0.80	0.40	C25/30	C25/30	C25/30	C25/30	129.01	1.80
56	5.00	20.00	20.00	0.10	0.80	0.40	1.00	0.40	0.80	0.40	C25/30	C25/30	C25/30	C25/30	129.48	1.81
57	5.00	20.00	20.00	0.10	0.80	0.40	0.80	0.40	0.85	0.40	C25/30	C25/30	C25/30	C25/30	127.58	1.77
58	5.00	20.00	20.00	0.10	0.80	0.40	0.80	0.40	0.90	0.40	C25/30	C25/30	C25/30	C25/30	127.58	1.77
59	5.00	20.00	20.00	0.10	0.80	0.40	0.80	0.40	0.95	0.40	C25/30	C25/30	C25/30	C25/30	127.58	1.77
60	5.00	20.00	20.00	0.10	0.80	0.40	0.80	0.40	1.00	0.40	C25/30	C25/30	C25/30	C25/30	127.58	1.77
61	5.00	20.00	20.00	0.10	0.80	0.40	0.80	0.40	1.10	0.40	C25/30	C25/30	C25/30	C25/30	127.58	1.77
62	5.00	20.00	20.00	0.10	0.80	0.40	0.80	0.40	1.15	0.40	C25/30	C25/30	C25/30	C25/30	127.58	1.77
63	5.00	20.00	20.00	0.10	0.80	0.40	0.80	0.40	1.20	0.40	C25/30	C25/30	C25/30	C25/30	127.58	1.77
64	5.00	20.00	20.00	0.10	0.80	0.30	0.80	0.40	0.80	0.40	C25/30	C25/30	C25/30	C25/30	170.26	1.88
65	5.00	20.00	20.00	0.10	0.80	0.35	0.80	0.40	0.80	0.40	C25/30	C25/30	C25/30	C25/30	146.26	1.82

66	5.00	20.00	20.00	0.10	0.80	0.45	0.80	0.40	0.80	0.40	C25/30	C25/30	C25/30	C25/30	112.70	1.73
67	5.00	20.00	20.00	0.10	0.80	0.50	0.80	0.40	0.80	0.40	C25/30	C25/30	C25/30	C25/30	100.65	1.70
68	5.00	20.00	20.00	0.10	0.80	0.55	0.80	0.40	0.80	0.40	C25/30	C25/30	C25/30	C25/30	90.74	1.68
69	5.00	20.00	20.00	0.10	0.80	0.60	0.80	0.40	0.80	0.40	C25/30	C25/30	C25/30	C25/30	82.48	1.65
70	5.00	20.00	20.00	0.10	0.80	0.65	0.80	0.40	0.80	0.40	C25/30	C25/30	C25/30	C25/30	75.52	1.63
71	5.00	20.00	20.00	0.10	0.80	0.70	0.80	0.40	0.80	0.40	C25/30	C25/30	C25/30	C25/30	69.58	1.62
72	5.00	20.00	20.00	0.10	0.80	0.40	0.80	0.30	0.80	0.40	C25/30	C25/30	C25/30	C25/30	125.63	1.57
73	5.00	20.00	20.00	0.10	0.80	0.40	0.80	0.35	0.80	0.40	C25/30	C25/30	C25/30	C25/30	126.60	1.68
74	5.00	20.00	20.00	0.10	0.80	0.40	0.80	0.45	0.80	0.40	C25/30	C25/30	C25/30	C25/30	128.55	1.86
75	5.00	20.00	20.00	0.10	0.80	0.40	0.80	0.50	0.80	0.40	C25/30	C25/30	C25/30	C25/30	129.52	1.96
76	5.00	20.00	20.00	0.10	0.80	0.40	0.80	0.55	0.80	0.40	C25/30	C25/30	C25/30	C25/30	130.49	2.04
77	5.00	20.00	20.00	0.10	0.80	0.40	0.80	0.60	0.80	0.40	C25/30	C25/30	C25/30	C25/30	131.46	2.13
78	5.00	20.00	20.00	0.10	0.80	0.40	0.80	0.65	0.80	0.40	C25/30	C25/30	C25/30	C25/30	132.43	2.21
79	5.00	20.00	20.00	0.10	0.80	0.40	0.80	0.70	0.80	0.40	C25/30	C25/30	C25/30	C25/30	133.40	2.29
80	5.00	20.00	20.00	0.10	0.80	0.40	0.80	0.40	0.80	0.30	C25/30	C25/30	C25/30	C25/30	110.22	1.75
81	5.00	20.00	20.00	0.10	0.80	0.40	0.80	0.40	0.80	0.35	C25/30	C25/30	C25/30	C25/30	118.95	1.76
82	5.00	20.00	20.00	0.10	0.80	0.40	0.80	0.40	0.80	0.45	C25/30	C25/30	C25/30	C25/30	136.10	1.78
83	5.00	20.00	20.00	0.10	0.80	0.40	0.80	0.40	0.80	0.50	C25/30	C25/30	C25/30	C25/30	144.51	1.80
84	5.00	20.00	20.00	0.10	0.80	0.40	0.80	0.40	0.80	0.55	C25/30	C25/30	C25/30	C25/30	152.82	1.81
85	5.00	20.00	20.00	0.10	0.80	0.40	0.80	0.40	0.80	0.60	C25/30	C25/30	C25/30	C25/30	161.03	1.82
86	5.00	20.00	20.00	0.10	0.80	0.40	0.80	0.40	0.80	0.65	C25/30	C25/30	C25/30	C25/30	169.15	1.83
87	5.00	20.00	20.00	0.10	0.80	0.40	0.80	0.40	0.80	0.70	C25/30	C25/30	C25/30	C25/30	177.16	1.84
88	5.00	20.00	20.00	0.10	0.80	0.40	0.80	0.40	0.80	0.40	C20/25	C25/30	C25/30	C25/30	123.30	1.80
89	5.00	20.00	20.00	0.10	0.80	0.40	0.80	0.40	0.80	0.40	C30/37	C25/30	C25/30	C25/30	136.08	1.71

90	5.00	20.00	20.00	0.10	0.80	0.40	0.80	0.40	0.80	0.40	C35/45	C25/30	C25/30	C25/30	136.08	1.68
91	5.00	20.00	20.00	0.10	0.80	0.40	0.80	0.40	0.80	0.40	C40/50	C25/30	C25/30	C25/30	144.51	1.65
92	5.00	20.00	20.00	0.10	0.80	0.40	0.80	0.40	0.80	0.40	C45/55	C25/30	C25/30	C25/30	148.70	1.63
93	5.00	20.00	20.00	0.10	0.80	0.40	0.80	0.40	0.80	0.40	C50/60	C25/30	C25/30	C25/30	152.87	1.60
94	5.00	20.00	20.00	0.10	0.80	0.40	0.80	0.40	0.80	0.40	C25/30	C20/25	C25/30	C25/30	131.81	1.79
95	5.00	20.00	20.00	0.10	0.80	0.40	0.80	0.40	0.80	0.40	C25/30	C30/37	C25/30	C25/30	119.81	1.74
96	5.00	20.00	20.00	0.10	0.80	0.40	0.80	0.40	0.80	0.40	C25/30	C35/45	C25/30	C25/30	116.24	1.73
97	5.00	20.00	20.00	0.10	0.80	0.40	0.80	0.40	0.80	0.40	C25/30	C40/50	C25/30	C25/30	112.86	1.72
98	5.00	20.00	20.00	0.10	0.80	0.40	0.80	0.40	0.80	0.40	C25/30	C45/55	C25/30	C25/30	109.65	1.71
99	5.00	20.00	20.00	0.10	0.80	0.40	0.80	0.40	0.80	0.40	C25/30	C50/60	C25/30	C25/30	106.60	1.70
100	5.00	20.00	20.00	0.10	0.80	0.40	0.80	0.40	0.80	0.40	C25/30	C25/30	C20/25	C25/30	127.58	1.78
101	5.00	20.00	20.00	0.10	0.80	0.40	0.80	0.40	0.80	0.40	C25/30	C25/30	C30/37	C25/30	127.57	1.75
102	5.00	20.00	20.00	0.10	0.80	0.40	0.80	0.40	0.80	0.40	C25/30	C25/30	C35/45	C25/30	127.57	1.74
103	5.00	20.00	20.00	0.10	0.80	0.40	0.80	0.40	0.80	0.40	C25/30	C25/30	C40/50	C25/30	127.57	1.74
104	5.00	20.00	20.00	0.10	0.80	0.40	0.80	0.40	0.80	0.40	C25/30	C25/30	C45/55	C25/30	127.57	1.73
105	5.00	20.00	20.00	0.10	0.80	0.40	0.80	0.40	0.80	0.40	C25/30	C25/30	C50/60	C25/30	127.56	1.72
106	5.00	20.00	20.00	0.10	0.80	0.40	0.80	0.40	0.80	0.40	C25/30	C25/30	C25/30	C20/25	127.73	1.77
107	5.00	20.00	20.00	0.10	0.80	0.40	0.80	0.40	0.80	0.40	C25/30	C25/30	C25/30	C30/37	127.27	1.77
108	5.00	20.00	20.00	0.10	0.80	0.40	0.80	0.40	0.80	0.40	C25/30	C25/30	C25/30	C35/45	127.11	1.77
109	5.00	20.00	20.00	0.10	0.80	0.40	0.80	0.40	0.80	0.40	C25/30	C25/30	C25/30	C40/50	126.96	1.77
110	5.00	20.00	20.00	0.10	0.80	0.40	0.80	0.40	0.80	0.40	C25/30	C25/30	C25/30	C45/55	126.80	1.77
111	5.00	20.00	20.00	0.10	0.80	0.40	0.80	0.40	0.80	0.40	C25/30	C25/30	C25/30	C50/60	126.65	1.77